

# High-temperature superconductivity in iron-based layered compounds\*

M V Sadovskii

DOI: 10.1070/PU2008v051n12ABEH006820

## Contents

<b>1. Introduction</b>	<b>1201</b>
1.1 Peculiarities of high-temperature superconductivity in copper oxides; 1.2 Other superconductors with unusual properties	
<b>2. Basic experimental data on new superconductors</b>	<b>1203</b>
2.1 Electrical properties and superconductivity; 2.2 Crystal structure and anisotropy; 2.3 Magnetic structure and phase diagram; 2.4 Specific heat; 2.5 NMR (NQR) and tunneling spectroscopy; 2.6 Optical properties; 2.7 Phonons and spin excitations: neutron spectroscopy; 2.8 Other experiments	
<b>3. Electronic spectrum and magnetism</b>	<b>1214</b>
3.1 Band structure (LDA); 3.2 ‘Minimal’ model; 3.3 Angle-resolved photoemission spectroscopy (ARPES); 3.4 Correlations (LDA + DMFT); 3.5 Spin ordering: localized or itinerant spins?	
<b>4. Mechanisms and types of pairing</b>	<b>1222</b>
4.1 Multiband superconductivity; 4.2 Electron–phonon mechanism; 4.3 Magnetic fluctuations	
<b>5. Conclusion: end of cuprate monopoly</b>	<b>1224</b>
<b>References</b>	<b>1225</b>

**From the Editorial Board.** An outstanding scientific discovery was made in early 2008 and extremely active research is now in progress. I am talking about a new class of superconductors. With this in mind, the Editorial Board requested one of its members (M V Sadovskii) to write a review article devoted to these new superconductors. During its preparation, however, two more reviews (one written by A L Ivanovskii, and the other by Yu A Izyumov and E Z Kurmaev) arrived in the editorial office. Encountering such a display of scientific activity in this field, and due to its obvious great significance, the Editorial Board took the exceptional decision to publish all three reviews in one and the same issue of the *Physics–Uspekhi* journal. The decision is all the more remarkable as the authors hold somewhat different viewpoints relative to the physics of the superconductors discovered. It is believed that such a decision will help our readers look deeply into this new area of research. At the same time, we recognize that our decision on the above matter is extraordinary and it is justified only by the topicality of the research in the field.

V L Ginzburg

M V Sadovskii Institute of Electrophysics, Ural Branch of the Russian Academy of Sciences,  
ul. Amundsena 106, 620016 Ekaterinburg, Russian Federation  
Tel. (7-343) 267 87 86. Fax (7-343) 267 87 94  
E-mail: sadovski@iep.uran.ru

Requested by the Editorial Board on 31 May 2008, received 31 October 2008  
*Uspekhi Fizicheskikh Nauk* 178 (12) 1243–1271 (2008)

DOI: 10.3367/UFNr.0178.200812b.1243

Translated by M V Sadovskii; edited by A Radzig

**Abstract.** Basic experimental data are presented for a new class of high-temperature superconductors — iron-based layered compounds of the types  $REOFeAs$  ( $RE = La, Ce, Nd, Pr, Sm, \dots$ ),  $AFe_2As_2$  ( $A = Ba, Sr, \dots$ ),  $AFeAs$  ( $A = Li, \dots$ ), and  $FeSe(Te)$ . The structure of electronic spectra in these compounds is discussed, including the correlation effects, as is the spectrum and role of collective excitations (phonons and spin waves). Basic models for describing various types of magnetic ordering and Cooper pairing are reviewed.

## 1. Introduction

The discovery of high-temperature superconductivity (HTSC) in copper oxides more than 20 years ago [1] stirred up profound interest and has led to the publication of thousands of experimental and theoretical papers. During this time, a number of reviews have been published in *Physics–Uspekhi*, which have been devoted to different aspects of superconductivity in cuprates and prospects for further progress in the growth of the critical temperature  $T_c$  of superconducting transition and appeared both immediately after this discovery [2–4] and much later [5–10]. The physics of HTSC and of a variety of new and unusual superconductors was discussed in a number of individual and collective monographs [11–14].

\* This review represents an expanded report under the same name delivered to the special meeting of the Editorial Board of the *Physics–Uspekhi* journal held on November 19, 2008 at the P N Lebedev Physical Institute, RAS in Moscow. This verbal issue of *Physics–Uspekhi* was timed to commemorate the 90th anniversary of the journal’s first publication in Russian and the 50th anniversary of the first issue translated into English. (*Editor’s note.*)

Unfortunately, despite these unprecedented efforts by researchers all over the world, the physical nature of high-temperature superconductivity in cuprates is still not completely understood. Basic difficulties here are attributed to the significant role of electronic correlations — in the opinion of the majority of authors cuprates make up strongly correlated systems, which leads to anomalies of their normal state (inapplicability of Fermi-liquid theory) and a wide spectrum of possible explanations for the microscopic mechanism of superconductivity — from relatively traditional [6, 9] to more or less exotic [12].

In this respect, the discovery in early 2008 of a new class of high-temperature superconductors, i.e., iron-based layered superconducting compounds [15], has attracted tremendous interest. This discovery has broken the cuprate ‘monopoly’ in the physics of HTSC compounds and revived hopes both of further progress in this field, related to the synthesis of new potential high-temperature superconductors, and of a deeper theoretical understanding of the mechanisms revealing themselves in HTSC. Naturally, a direct comparison between superconductivity in cuprates and new iron-based superconductors holds out the promise of identifying common peculiarities of these systems, which are relevant for high values of  $T_c$ , as well as important differences and properties not directly related to the phenomenon of high-temperature superconductivity and, in fact, complicating its theoretical interpretation.

The aim of the present review is to give a short introduction to the physics of new iron-based layered superconductors and to compare their properties with well-established facts concerning HTSC in copper oxides. Progress in this field has been rather spectacular and rapid, so that this review is in no sense exhaustive.<sup>1</sup> Nevertheless, the author hopes that it will serve as an elementary introduction to this new field of research and may help promote deeper studies of original papers.

### 1.1 Peculiarities of high-temperature superconductivity in copper oxides

At present, dozens of HTSC compounds based on copper oxides are known to have superconducting transition temperature  $T_c$  exceeding 24 K [16]. In Table 1 we present critical temperatures for a number of the most ‘popular’ cuprates.

**Table 1.** Superconducting transition temperatures in copper oxides.

Compound*	$T_c$ , K
HgBa <sub>2</sub> Ca <sub>2</sub> Cu <sub>3</sub> O <sub>8+δ</sub>	134
Tl <sub>2</sub> Ca <sub>2</sub> Ba <sub>2</sub> Cu <sub>3</sub> O <sub>10</sub>	127
YBa <sub>2</sub> Cu <sub>3</sub> O <sub>7</sub>	92
Bi <sub>2</sub> Sr <sub>2</sub> CaCu <sub>2</sub> O <sub>8</sub>	89
La <sub>1.83</sub> Sr <sub>0.17</sub> CuO <sub>4</sub>	37
Nd <sub>1.85</sub> Ce <sub>0.15</sub> CuO <sub>4</sub>	24

\*  $T_c$  of HgBa<sub>2</sub>Ca<sub>2</sub>Cu<sub>3</sub>O<sub>8+δ</sub> reaches ~ 150 K under pressure.

<sup>1</sup> Suffice it to say that during the first six months of the studies of new superconductors about 600 original papers (preprints) were published. Obviously, in this review it is not even possible just to cite all these works, and our choice of citations is rather subjective. The author apologizes in advance to those authors of important papers which remained outside our reference list, as this is attributed to an obvious limitation on the size of the review and the author’s own ignorance.

More than 20 years of experience has led to a quite deep understanding of the nature of superconductivity in these systems. It is clear, for example, that HTSC in cuprates is not connected with some ‘essentially new’ physics, which is different in comparison with other superconductors, superfluid Fermi liquids like He<sup>3</sup>, nucleons in atomic nuclei or nuclear matter in neutron stars, dilute Fermi gases with Cooper pairing actively studied at present, or even the hypothetical ‘color’ superconductivity of quarks.

In this respect, let us list below

#### What we definitely know about cuprates:

- *The nature of superconductivity in cuprates*  $\rightleftharpoons$  *Cooper pairing.*

- (1) This pairing is anisotropic and of the d-type, so that the energy gap acquires zeroes at the Fermi surface:  $\Delta \cos 2\phi$ , where  $\phi$  is the polar angle determining momentum direction in the two-dimensional Brillouin zone.

- (2) The size of Cooper pairs (coherence length at zero temperature  $T = 0$ ) is relatively small:  $\xi_0 \sim (5-10)a$ , where  $a$  is the lattice constant in the CuO<sub>2</sub> plane.

- *There exists a relatively well-defined (at least in part of the Brillouin zone) Fermi surface; in this sense these systems are metals.*

- *However, appropriate stoichiometric compounds constitute antiferromagnetic insulators — their superconductivity is realized close to the Mott metal–insulator phase transition (controlled by composition) induced by strong electronic correlations.*

- *Strong anisotropy of all electronic properties is observed — conductivity (and superconductivity) is realized mainly within CuO<sub>2</sub> layers (quasi-two-dimensionality!).*

At the same time, many things are still not understood. Accordingly, we may list

#### What we do not really know about cuprates:

- *Mechanism of Cooper pairing (a ‘glue’ ensuring a formation of Cooper pairs).*

Possible variants:

- (1) Electron–phonon mechanism.

- (2) Spin fluctuations.

- (3) Exchange–RVB, SO(5), or something more ‘exotic’.

The difficulties of choice here are mainly due to the unclear

- *Nature of the normal state.*

- (1) Is Fermi-liquid theory (Landau) valid here?

- (2) Or is some more complicated scenario realized, like a ‘marginal’ or ‘bad’ Fermi liquid?

- (3) Possible also is some variant of a Luttinger liquid, essentially different from a Fermi liquid.

- (4) Still mysterious is the nature of the pseudogap state.

- (5) Not completely clear is the role of internal disorder and local inhomogeneities.

Of course, we observe here continuous, though slow, progress. For example, most researchers are now leaning towards the spin-fluctuation (nonphonon) mechanism of pairing. The pseudogap state is most likely connected with fluctuations of some competing (with superconductivity) order parameter (antiferromagnetic or charged) [7, 17, 18]. The Fermi-liquid description is apparently applicable in most parts of the Brillouin zone, where the Fermi surface remains not ‘destroyed’ by pseudogap fluctuations, etc. However, a consensus in the HTSC community is still absent, which is obviously related to the complicated nature of these systems, attributed first and foremost to strong electronic correlations which control this nature and impede theoretical under-

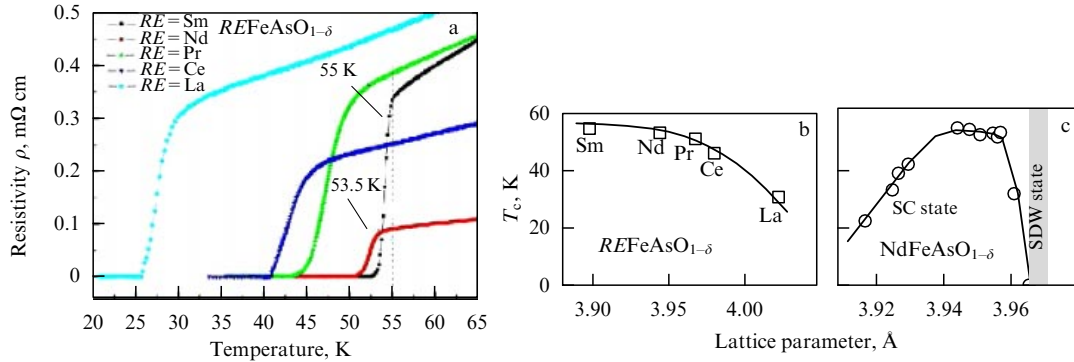


**Figure 1.** (a) Resistivity behavior in REOFeAs ( $RE = \text{La, Ce, Pr, Nd, Sm}$ ) close to the superconducting (SC) transition. (b, c) Dependence of  $T_c$  (the onset of transition) on the value of the lattice constant [33].

standing. Just because of that, the discovery of a new class of HTSC compounds holds out definite hope, as new possibilities of HTSC studies in completely different systems appear, and where some of these difficulties may just be absent.

## 1.2 Other superconductors with unusual properties

Obviously, during all the years since the discovery of HTSC in cuprates active efforts have continued in the search for new compounds with potentially high superconducting transition temperatures. A number of systems discovered during this search are listed in Table 2.

**Table 2.** Superconducting transition temperatures in some ‘unusual’ superconductors.

Compound	$T_c$ , K
MgB <sub>2</sub>	39
RbCs <sub>2</sub> C <sub>60</sub>	33
K <sub>3</sub> C <sub>60</sub>	19
Sr <sub>2</sub> RuO <sub>4</sub>	1.5

Despite the obvious interest from the viewpoint of physics and the unusual properties of some of these systems, there has been no significant progress in this area. This is mainly due to the fact that all the systems listed in Table 2 are, in some sense, ‘exceptional’ — none is representative of a wide class of compounds with the possibility of changing system properties (parameters) in a wide range, as in cuprates. All these systems have been studied in detail, and summaries of these studies can be found in the relevant reviews [19–23]. In fact, these studies have added very little to our understanding of the superconductivity of cuprates. Up to now, there has been a kind of ‘cuprate monopoly’ in the physics of ‘real’ HTSC materials with a great potential for further studies and the search for compounds with even higher values of  $T_c$  and practical applications.<sup>2</sup>

## 2. Basic experimental data on new superconductors

### 2.1 Electrical properties and superconductivity

**2.1.1 REOFeAs ( $RE = \text{La, Ce, Pr, Nd, Sm, ...}$ ) system.** The discovery of superconductivity with  $T_c = 26$  K in

LaO $_{1-x}$ F $_x$ FeAs ( $x = 0.05–0.12$ ) [15] was preceded by studies of the electrical properties of a number of oxypnictides like LaOMPn ( $M = \text{Mn, Fe, Co, Ni, and Pn} = \text{P, As}$ ) gone with the discovery of superconductivity in LaOFeP with  $T_c \sim 5$  K [24] and LaONiP with  $T_c \sim 3$  K [25], which has not attracted much attention from the HTSC community. This situation has changed sharply since Ref. [15] appeared, and shortly afterwards many papers followed (see, e.g., Refs [26–35]), where this discovery was confirmed, and the substitution of lanthanum by a number of other rare earths, according to the simple chemical formula  $(RE)^{+3}O^{-2}Fe^{+2}As^{-3}$ , has led to more than a doubling of  $T_c$  up to values on the order of 55 K in systems based upon NdOFeAs and SmOFeAs, with electron doping effected through the addition of fluorine or creation of an oxygen deficit, or hole doping implemented by partial substitution of the rare earth (e.g., La by Sr) [36]. Note also work [37] where the record values of  $T_c \sim 55$  K were achieved by partial substitution of Gd in GdOFeAs by Th, which, according to the authors, also corresponded to electron doping. In these early works, different measurements of electrical and thermodynamic properties of superconductors were performed on polycrystalline samples.

Figure 1a taken from Ref. [33] demonstrate typical temperature dependences of electric resistivity in different REOFeAs compounds. It can be seen that for most of these compounds  $T_c$  lies within the interval 40–50 K, while the LaOFeAs system slightly drops out of this series, with its significantly lower transition temperature of  $\sim 25$  K. In this respect, we can mention Ref. [34] in which a synthesis of this system under high pressure was reported, producing samples with  $T_c$  (the onset of the superconducting transition) on the order of 41 K. In Ref. [38], an analogous increase in  $T_c$  in such a system was achieved under an external pressure of  $\sim 4$  GPa. Probably, this last result is characteristic only of the La system, as a further increase in pressure leads to a drop in  $T_c$ , while in other systems (e.g., Ce-based systems)  $T_c$  lowers with an increase in external pressure from the very beginning (see, e.g., Ref. [39, 40]).

In many papers, the growth in  $T_c$  induced by La replacement with other rare earths (with a smaller ion radius) is often attributed to ‘chemical’ pressure, which is illustrated, for instance, by the qualitative dependence of  $T_c$  on lattice spacing, depicted in Fig. 1b [33]. At the same time, Fig. 1c taken from the same work shows that lattice compression leads to a growth in  $T_c$  only up to a certain limit, and after that  $T_c$  drops (compare this evidence with

<sup>2</sup> Surely, when we speak about practical applications we should not underestimate the prospects of the MgB<sub>2</sub> compound.

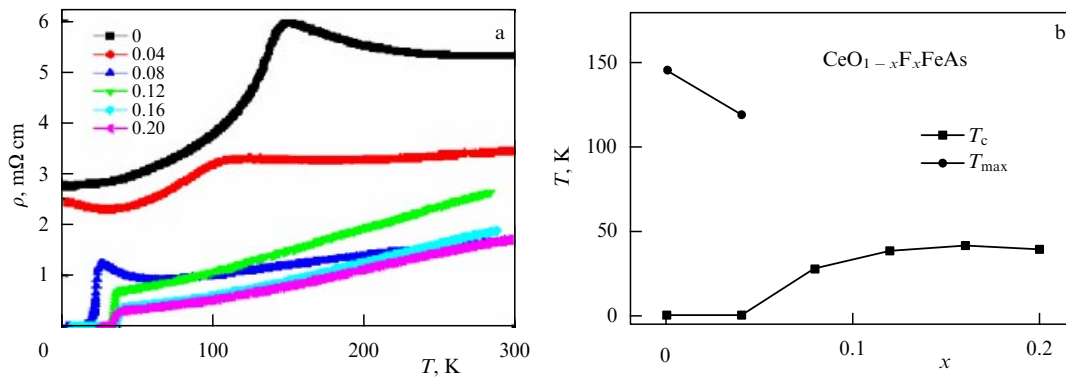


**Figure 2.** (a) Temperature dependence of resistivity in CeO<sub>1-x</sub>F<sub>x</sub>FeAs for different compositions  $x$  given on the graph. (b) Phase diagram showing the superconducting region and concentration dependence of high-temperature anomaly  $T_{max}$  of resistivity, associated with the SDW transition [30].

the results of the high-pressure experiments mentioned above).

In a wider temperature interval, the typical temperature behavior of resistivity is illustrated by the data for CeO<sub>1-x</sub>F<sub>x</sub>FeAs shown in Fig. 2a (taken from Ref. [30]). It can be seen that the prototype system CeOFeAs is characterized by a *metallic* behavior of resistivity up to the lowest temperatures achieved, with the characteristic anomaly in the vicinity of  $T \sim 145$  K and a sharp drop in resistivity at lower temperatures. The metallic nature of prototype REOFeAs systems contrasts with the insulating nature of stoichiometric cuprates. After doping, for example, by fluorine, the value of resistivity drops, and its anomaly becomes less pronounced and disappears at higher dopings, where superconductivity appears. The highest value of  $T_c = 41$  K is achieved for  $x = 0.16$ , and the resulting F-concentration phase diagram is displayed in Fig. 2b. The high-temperature anomaly of resistivity in prototype and slightly doped systems in most of the works was attributed to a structural phase transition and (or) subsequent spin density wave (SDW) transition, while the degradation of the SDW state under doping is usually connected with the breaking of ‘nesting’ of the Fermi surfaces (cf. below). This behavior of resistivity is rather typical and is observed in all REOFeAs systems (see, e.g., Ref. [32]), which are for the sake of brevity now called 1111-systems.

In fact, the recently synthesized compound Sr(Ca)FFeAs belongs to the same class [41, 42]. Here, the typical SDW anomaly of resistivity is also observed in the vicinity of 175 K. Further doping of this system with Co leads to the appearance of superconductivity with  $T_c \sim 5$  K [43], while in Sr<sub>1-x</sub>La<sub>x</sub>FFeAs, a superconducting transition with  $T_c = 36$  K [44] was obtained.

**2.1.2 AFe<sub>2</sub>As<sub>2</sub> (A = Ba, Sr, ...) system.** A simpler (structurally and chemically) class of iron-based superconductors was discovered in Ref. [45] by the synthesis of the Ba<sub>1-x</sub>K<sub>x</sub>Fe<sub>2</sub>As<sub>2</sub> compound, where superconductivity with  $T_c = 38$  K was observed for  $x = 0.4$ . The relevant data on the temperature dependence of resistivity are given in Fig. 3 [45].

In the prototype BaFe<sub>2</sub>As<sub>2</sub> compound, temperature dependence of resistivity demonstrates typically metallic behavior with a characteristic anomaly in the vicinity of  $T \sim 140$  K, which is connected to a spin density wave (SDW) and structural phase transitions (cf. below). Accord-

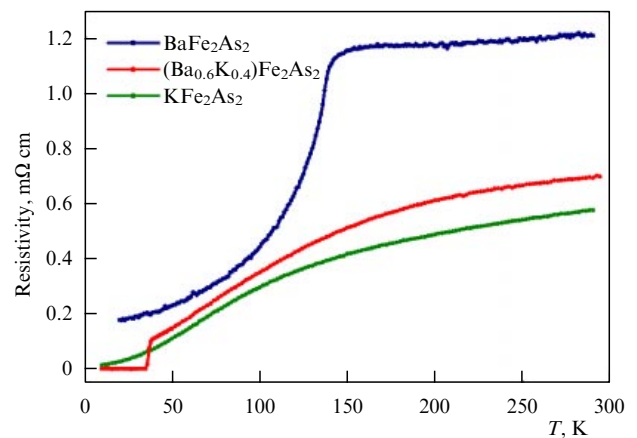


**Figure 3.** Temperature dependence of resistivity in Ba<sub>1-x</sub>K<sub>x</sub>Fe<sub>2</sub>As<sub>2</sub> for different compositions  $x$  shown on the graph [45].

ing to the simple chemical formula Ba<sup>+2</sup>(Fe<sup>+2</sup>)<sub>2</sub>(As<sup>-3</sup>)<sub>2</sub>, the partial substitution of K<sup>+1</sup> for Ba<sup>+2</sup> leads to hole doping which suppresses SDW transition and gives rise to superconductivity in a certain concentration interval. Obviously, these results are quite similar to those quoted above for REOFeAs (1111) systems.

In Ref. [46], a similar behavior was observed in Sr<sub>1-x</sub>K<sub>x</sub>Fe<sub>2</sub>As<sub>2</sub> with maximal  $T_c \sim 38$  K, while in Ref. [47] systems like AFe<sub>2</sub>As<sub>2</sub> with A = K, Ca, K/Sr, Ca/Sr were studied, and electron doping by Sr of compounds with A = K and A = Cs produced values of  $T_c \sim 37$  K followed by SDW transition. This new class of Fe-based HTSCs is sometimes denoted for brevity as 122-systems.

Notice also the interesting paper [48] where superconductivity with  $T_c$  up to 29 K was obtained in the prototype (undoped) BaFe<sub>2</sub>As<sub>2</sub> and SrFe<sub>2</sub>As<sub>2</sub> compounds under external pressure, but only in a limited interval of pressures. Superconductivity also appears under electron doping of these systems by Co [49].

**2.1.3 AFeAs (A = Li, ...) system.** One more type of Fe-based superconductors is represented by the Li<sub>1-x</sub>FeAs (111) system, where superconductivity appears at  $T_c \sim 18$  K [50, 51]. Up to now there have been few works on this system; however, it is clear that it is quite similar to 1111- and 122-systems and is rather promising in the sense of comparing its properties with those of the other systems discussed above.

**2.1.4 FeSe(Te) system.** Finally, rather unexpectedly, superconductivity was discovered in the very ‘simple’  $\alpha$ -FeSe<sub>x</sub> ( $x < 1$ ) system [52] with  $T_c = 8$  K, reaching 27 K under a pressure of 1.48 GPa [53]. Later on, the system Fe(Se<sub>1-x</sub>Te<sub>x</sub>)<sub>0.82</sub> was also studied, and the maximum value of  $T_c = 14$  K was achieved for  $0.3 < x < 1$  [54]. Here, there are still very few detailed studies, though it is quite clear that the electronic structures of these systems are again similar to those discussed above, so that in the nearest future we can expect many papers devoted to the comprehensive studies of their electronic properties.

**2.1.5 Search for new systems.** Naturally, at present an active search for other similar systems is underway with the hope of obtaining even higher values of  $T_c$ . Up to now, excepting the domain of FeAs-based systems, successes have been rather modest. We shall mention only a few works where new superconductors were synthesized.

We have already mentioned compounds like LaOFeAs with  $T_c \sim 5$  K [24] and LaONiP with  $T_c \sim 3$  K [25], which are representatives of the same class of superconducting oxypnictides (1111) as the whole series of REOFeAs. Superconductivity with  $T_c \sim 4$  K was discovered in the LaO<sub>1- $\delta$</sub> NiBi compounds [55], while in GdONiBi and Gd<sub>0.9</sub>Sr<sub>0.1</sub>ONiBi, the value of  $T_c \sim 0.7$  K was found in Ref. [56]. Transition temperature  $T_c \sim 2.75$  K was obtained in LaO<sub>1-x</sub>F<sub>x</sub>NiAs [57].

In the class of 122-systems, the value of  $T_c \sim 0.7$  K was revealed in BaNi<sub>2</sub>As<sub>2</sub> [58].

An interesting new system, La<sub>3</sub>Ni<sub>4</sub>P<sub>4</sub>O<sub>2</sub>, with a different crystal structure demonstrated superconductivity close to  $T_c \sim 2.2$  K [59]. In this work, a number of promising systems of the same type were also discussed.

Certainly, none of these results is very exciting. However, there are a rather large number of systems somehow similar to already known FeAs-based compounds where we can also expect the manifestation of superconductivity at fairly high temperatures. A wide set of promising compounds was considered in Ref. [60].

## 2.2 Crystal structure and anisotropy

The crystal structure of BaFe<sub>2</sub>As<sub>2</sub> and LaOFeAs compounds and their analogs corresponds to tetragonal symmetry and space groups  $I4/mmm$  and  $P4/nmm$ , respectively. Both compounds are formed by layers of (FeAs)<sup>-</sup> with covalent bonding, interlaced by layers of Ba<sub>0.5</sub><sup>2+</sup> or (LaO)<sup>+</sup>, while interlayer bonding is ionic. Fe<sup>2+</sup> ions are surrounded by four ions of As, which form tetrahedra. The general view of crystal structures of LaOFeAs and BaFe<sub>2</sub>As<sub>2</sub> is illustrated in Fig. 4. The layered (quasi-two-dimensional) nature of these compounds is similar to that of HTSC cuprates. At 140 K, BaFe<sub>2</sub>As<sub>2</sub> undergoes a structural phase transition from a tetragonal ( $I4/mmm$ ) to an orthorhombic ( $Fmmm$ ) structure [61]. An analogous transition also takes place in LaOFeAs at 150 K:  $P4/nmm$  (tetragonal)  $\rightarrow$   $Cmma$  (orthorhombic) [62]. Experimental atomic positions in BaFe<sub>2</sub>As<sub>2</sub> are as follows: Ba (0, 0, 0), Fe (0.5, 0, 0.25), and As (0, 0,  $z$ ). For LaOFeAs, these are: La (0.25, 0.25,  $z$ ), Fe (0.75, 0.25, 0.5), As (0.25, 0.25,  $z$ ), and O (0.75, 0.25, 0). The rest of crystallographic data for both compounds in tetragonal phase are given in Table 3. It is seen that in BaFe<sub>2</sub>As<sub>2</sub> the Fe–As distance is smaller than in LaOFeAs. Thus, in BaFe<sub>2</sub>As<sub>2</sub> we can expect stronger Fe- $d$ –As- $p$  hybridization in comparison with LaOFeAs and, correspondingly, a larger  $d$ -band width for Fe. Similarly, the

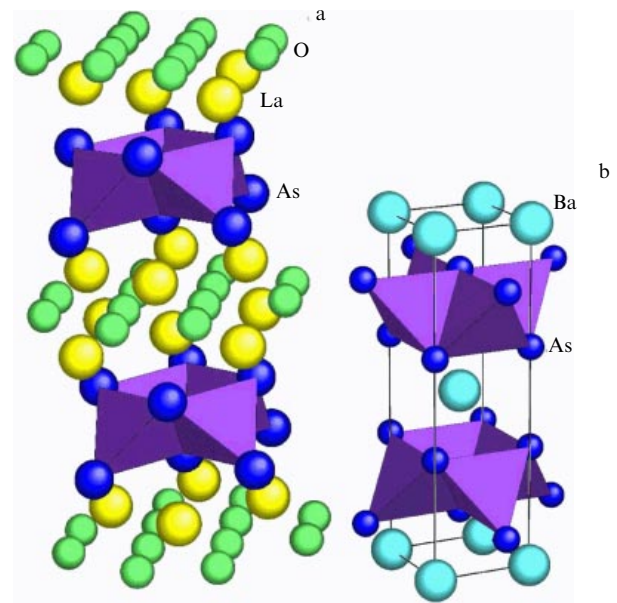


**Figure 4.** Crystal structures of LaOFeAs (a) and BaFe<sub>2</sub>As<sub>2</sub> (b). FeAs tetrahedra form two-dimensional layers surrounded by layers of LaO or Ba. Iron ions inside the tetrahedra form a square lattice.

**Table 3.** Structural data for BaFe<sub>2</sub>As<sub>2</sub> and LaOFeAs.

Parameters	BaFe <sub>2</sub> As <sub>2</sub> [45]	LaOFeAs [15]
Group	$I4/mmm$	$P4/nmm$
$a$ , Å	3.9090(1)	4.03533(4)
$c$ , Å	13.2122(4)	8.74090(9)
$z_{\text{La}}$	—	0.14154(5)
$z_{\text{As}}$	0.3538(1)	0.6512(2)
Ba–As, Å	$3.372(1) \times 8$	—
La–As, Å	—	$3.380 \times 4$
Fe–As, Å	$2.388(1) \times 4$	$2.412 \times 4$
Fe–Fe, Å	$2.764(1) \times 4$	$2.853 \times 4$
As–Fe–As, deg.	$109.9(1)^\circ$	$113.6^\circ$
	$109.3(1)^\circ$	$107.5^\circ$

distance between adjacent Fe atoms within the FeAs layers in BaFe<sub>2</sub>As<sub>2</sub> is also significantly smaller than in LaOFeAs (and related compounds). After the phase transition of BaFe<sub>2</sub>As<sub>2</sub> into an orthorhombic structure, the four (initially equal) Fe–Fe distances are broken up into two pairs of bonds with lengths of 2.808 and 2.877 Å. Moreover, two As–Fe–As angles are significantly different in the LaOFeAs system ( $113.6^\circ$  and  $107.5^\circ$ ) and very close in BaFe<sub>2</sub>As<sub>2</sub> ( $\sim 109^\circ$ ). Such differences in the nearest neighborhood of Fe ions should lead to appropriate distinctions in their electronic structure.

Doping of prototype REOFeAs compounds by fluorine (or by the creation of an oxygen deficit) or BaFe<sub>2</sub>As<sub>2</sub> by substitution of K for Ba (Sr), etc., leads to the suppression of transition from the tetragonal to orthorhombic structure and the appearance of superconductivity in the tetragonal phase.

Recently, the crystal structure of the LiFeAs compound was also refined [51]. LiFeAs forms a tetragonal structure with space group  $P4/nmm$  and lattice parameters  $a = 3.7914(7)$  Å,  $c = 6.364(2)$  Å. The experimentally determined atomic positions are as follows: Fe(2b) (0.75, 0.25, 0.5), Li(2c) (0.25, 0.25,  $z_{\text{Li}}$ ), As(2c) (0.25, 0.25,  $z_{\text{As}}$ ),  $z_{\text{As}} = 0.26351$ , and  $z_{\text{Li}} = 0.845915$  [51]. The crystal structure of LiFeAs is

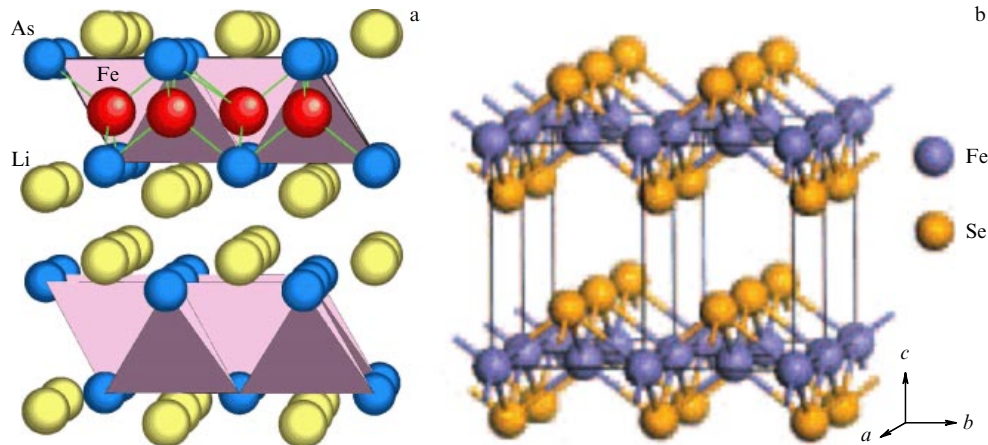


**Figure 5.** (a) Crystal structure of LiFeAs. FeAs tetrahedra form two-dimensional layers separated by layers of Li ions. (b) Crystal structure of  $\alpha$ -FeSe.

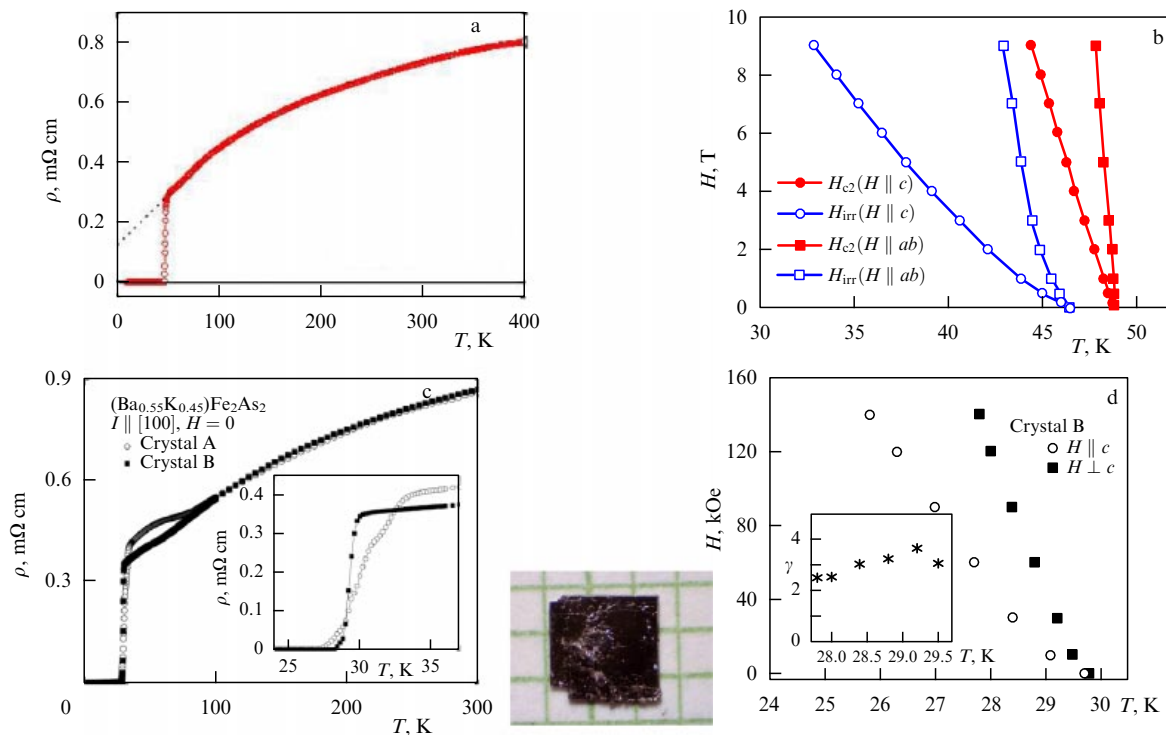


**Figure 6.** (a) Superconducting transition and (b) anisotropic behavior of the upper critical field  $H_{c2}$  (and irreversibility field  $H_{irr}$ ) in a single crystal of NdO<sub>0.82</sub>Fe<sub>0.18</sub>FeAs [64]. (c) Superconducting transition and (d) anisotropic behavior of the upper critical field  $H_{c2}$  in single crystals of Ba<sub>1-x</sub>K<sub>x</sub>FeAs [65], where in the insets we also show a weak temperature dependence of the anisotropy of  $H_{c2}$ . Shown in the photo is a typical single crystal of Ba<sub>1-x</sub>K<sub>x</sub>Fe<sub>2</sub>As<sub>2</sub>.

illustrated in Fig. 5a and is again characterized by clearly defined layering, which suggests quasi-two-dimensional electronic properties and is clearly analogous to the structure of LaOFeAs [15] and BaFe<sub>2</sub>As<sub>2</sub> [61]. Most important Fe–Fe and Fe–As distances are 2.68 and 2.42 Å, respectively. At present, this structure is most spatially compact among similar compounds. As–Fe–As angles in LiFeAs have the values of  $\sim 103.1^\circ$  and  $\sim 112.7^\circ$ , which can also lead to some fine differences in electronic structure of LiFeAs in comparison with LaOFeAs and BaFe<sub>2</sub>As<sub>2</sub>.

The crystal structure of  $\alpha$ -FeSe is especially simple — it forms the layered tetragonal phase (like PbO) with a square sublattice of Fe and space group  $P4/nmm$ . The  $\alpha$ -FeSe crystal consists of layers of FeSe<sub>4</sub> edge-sharing tetrahedra, as shown

in Fig. 5b. Experimentally determined lattice constants are as follows [52]:  $a = 3.7693(1)$  Å,  $c = 5.4861(2)$  Å for FeSe<sub>0.82</sub>, and  $a = 3.7676(2)$  Å,  $c = 5.4847(1)$  Å for FeSe<sub>0.88</sub>. An analogy with oxypnictides like REOFeAs and systems like BaFe<sub>2</sub>As<sub>2</sub> is obvious. At  $T \sim 105$  K, this system undergoes a structural phase transition from a tetragonal to a triclinic phase (group P-1) [52].

Up to now, only very small single crystals of 1111-compounds have been successfully synthesized ( $\sim 100 \times 100 \mu\text{m}^2$ ) (see, e.g., Refs [63, 64]). The situation with 122-systems is much better, where almost immediately single crystals of millimeter sizes were obtained (see Fig. 6) [65]. Thus, most of the measurements in what follows were made on single crystals of this system

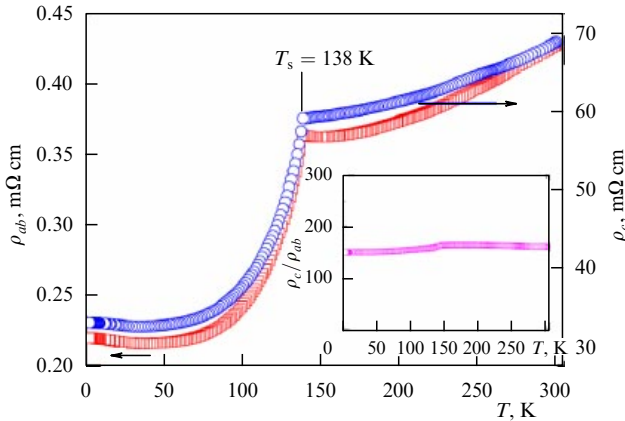


**Figure 7.** Temperature dependences of resistivity  $\rho_{ab}$  in the  $ab$  plane and of transverse resistivity  $\rho_c$  in the orthogonal direction in a single crystal of  $\text{BaFe}_2\text{As}_2$  [67]. Shown in the inset is the temperature dependence of the resistivity anisotropy.

(though for 1111-systems a number of interesting studies on single crystals were also performed). Recently, rather small single crystals ( $\sim 200 \times 200 \mu\text{m}^2$ ) of  $\alpha$ -FeSe with  $T_c \sim 10$  K have also been obtained [66], but detailed physical measurements on this system have yet to be done.

Typical results of measurements on single crystals of 1111 [64] and 122 [65] systems are given in Fig. 6. In particular, the anisotropy of the upper critical field  $H_{c2}$  testifies to the quasi-two-dimensional nature of the electronic subsystem in these superconductors, which is already evident from their crystal structure. At the same time, we can see that this anisotropy of critical fields is not too large.

In Fig. 7 taken from Ref. [67] we depicted the temperature dependences of resistivity  $\rho_{ab}$  in the  $ab$  plane and of transverse resistivity  $\rho_c$  in the orthogonal direction for a prototype (undoped)  $\text{BaFe}_2\text{As}_2$  system [67]. It can be seen that the resistivity anisotropy exceeds  $10^2$ , which confirms the quasi-two-dimensional nature of the electronic properties of this system. This anisotropy is significantly larger than the value which can be expected from simple estimates<sup>3</sup> based on the above-mentioned anisotropy of  $H_{c2}$ . However, we must stress that data on the anisotropy of the resistivity of superconducting samples in Refs [65, 67] are absent. In the data given in Fig. 7 we can also clearly see an anomaly in the temperature dependence of resistivity at  $T_s = 138$  K, which is connected with the antiferromagnetic (SDW) transition.

The question concerning the anisotropy of electronic properties has become more acute after measurements in Ref. [68] of  $H_{c2}$  in single crystals of  $\text{Ba}_{1-x}\text{K}_x\text{Fe}_2\text{As}_2$  were performed in a much wider temperature interval than in Ref. [65], up to the field values on the order of  $\sim 60$  T. According to Ref. [68], the anisotropy of  $H_{c2}$  is observed only in the relatively narrow temperature interval close to  $T_c$ , changing to almost isotropic behavior as the temperature lowers.

### 2.3 Magnetic structure and phase diagram

As mentioned above, with lowering temperature the prototype (undoped) 1111 and 122 compounds undergo a structural transition accompanied by a simultaneous or later

antiferromagnetic transition (probably of the SDW type). Direct confirmation of this picture was obtained in neutron scattering experiments. The first results for an  $\text{LaOFeAs}$  system were given in Ref. [69]. It was discovered that the structural transition in this compound (according to Ref. [69], from the orthorhombic  $P4/nmm$  to the monoclinic  $P112/n$  structure, which differs from the evidence of other authors [62]) takes place at  $T \sim 150$  K (where an anomaly in the temperature dependence of resistivity is observed), and afterwards antiferromagnetic ordering appears at  $T \sim 134$  K.

Shown in Fig. 8a are the antiferromagnetic structure obtained in these experiments, as well as the temperature dependence of the square of the magnetic moment at the Fe site. The value of this moment is not larger than  $0.36(5) \mu_B$ . We see that spin ordering in the  $ab$  plane takes the form of characteristic chains of ferromagnetically oriented spins with opposite spin orientations in neighboring chains (stripes). Along the  $c$ -axis there occurs typical period doubling.

In Fig. 8b we compare the magnetic structures in the  $\text{CuO}_2$  plane of cuprates and in the FeAs plane of new FeAs-based superconductors. Analogies and significant distinctions alike can clearly be seen. Both structural and antiferromagnetic transitions in FeAs planes are suppressed by doping, similarly to the situation in cuprates. At the same time, it should be stressed that the antiferromagnetic phase of cuprates is an insulator, while it remains metallic in FeAs-based superconductors, as is clearly seen from the data on resistivity quoted above.

The phase diagram of new superconductors (with a changing concentration of the doping element) is also significantly different from that of cuprates. Shown in Fig. 9 is the phase diagram for the  $\text{LaO}_{1-x}\text{F}_x\text{FeAs}$  system, obtained in Ref. [70] from  $\mu\text{SR}$  experiments. It can be seen that the temperatures of structural and magnetic transitions are clearly separated, while the superconducting region does not overlap with the antiferromagnetic region.

An analogous phase diagram for the  $\text{CeO}_{1-x}\text{F}_x\text{FeAs}$  compound, obtained in Ref. [71] from neutron scattering data, is drawn in Fig. 9b. According to this work, a structural tetra-ortho transition ( $P4/nmm \rightarrow Cmma$ ) is also well resolved from the antiferromagnetic transition, which takes place at lower temperatures, while the superconducting region does not overlap with the region of antiferromagnetic ordering on Fe. At the same time, the magnetic structure of  $\text{CeO}_{1-x}\text{F}_x\text{FeAs}$ , demonstrated in Fig. 10, is somewhat different from that of  $\text{LaO}_{1-x}\text{F}_x\text{FeAs}$  (obtained by the same team [69]). In the FeAs plane we again have a stripe structure similar to that in  $\text{LaOFeAs}$ , but spins on the adjacent planes are parallel and in consequence there occurs no period doubling along the  $c$ -axis. The value of the magnetic moment on Fe is as high as  $0.8(1) \mu_B$  at 40 K, which is roughly twice as large as in  $\text{LaOFeAs}$ . Also in Ref. [71], a magnetic structure due to Ce spin ordering was determined at  $T = 1.7$  K. According to this work, a strong correlation between the spins of Fe and Ce appears already at temperatures below 20 K. It should be noted that spin ordering on rare-earth ions in an  $\text{REOFeAs}$  series typically takes place at temperatures on the order of a few K, which are nearly an order of magnitude higher than similar temperatures in cuprates like  $\text{REBa}_2\text{Cu}_3\text{O}_{7-\delta}$  [72], giving evidence of a significantly stronger interaction between these spins. The general picture of spin ordering in  $\text{CeO}_{1-x}\text{F}_x\text{FeAs}$  is portrayed in Fig. 10.

Notice that data obtained by neutron scattering are still sometimes contradictory. For example, in Ref. [73], where the

<sup>3</sup> The anisotropy of  $H_{c2}$  is usually on the order of the square root of the resistivity anisotropy.

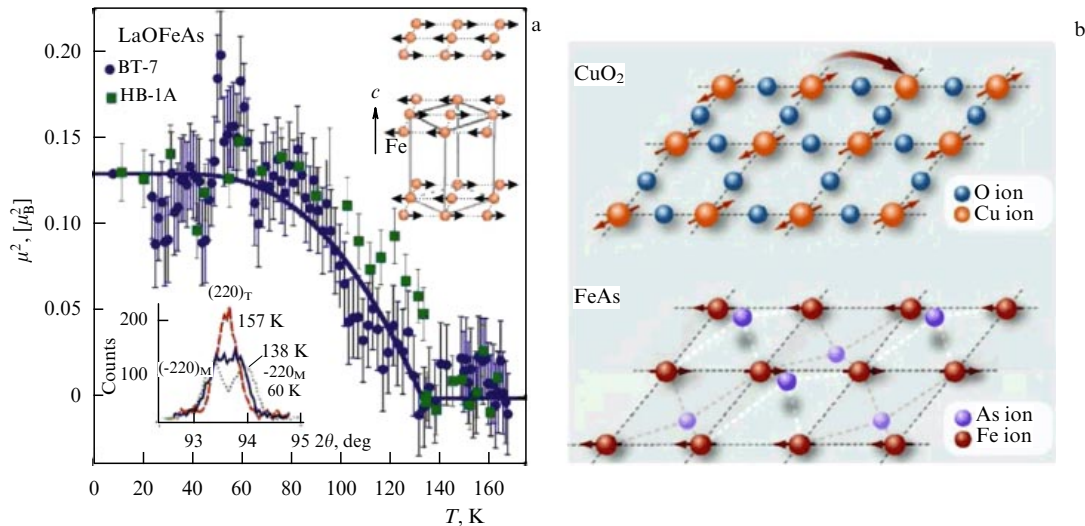


**Figure 8.** (a) Temperature dependence of the square of the magnetic moment at the Fe site in LaOFeAs obtained by neutron scattering (data from two spectrometers denoted as BT-7 and HB-1A) [69]. Shown in the inset in the upper right corner is the experimentally determined antiferromagnetic structure in the  $\sqrt{2}a \times \sqrt{2}b \times 2c$  lattice cell. Distortion of the nuclear scattering peak shown in the inset in the lower left corner suggests that structural transition precedes magnetic transition. (b) Comparison of antiferromagnetic ordering in the  $\text{CuO}_2$  plane of cuprates and in the FeAs plane of new superconductors.

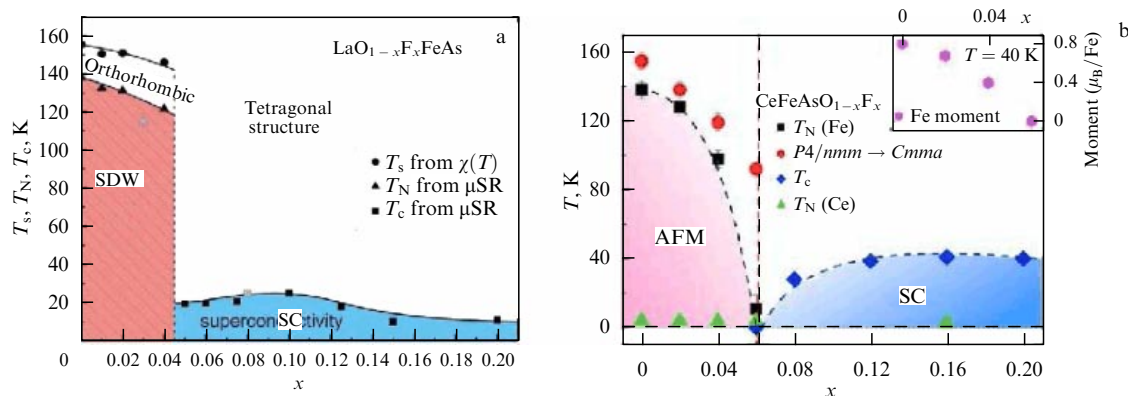


**Figure 9.** (a) Phase diagram of  $\text{LaO}_{1-x}\text{F}_x\text{FeAs}$  obtained from  $\mu\text{SR}$  experiments [70]. It portrays the concentration dependences of critical temperatures of superconducting ( $T_c$ ), magnetic ( $T_N$ ), and structural ( $T_s$ ) transitions (determined from resistivity measurements). (b) Phase diagram of the  $\text{CeO}_{1-x}\text{F}_x\text{FeAs}$  system obtained from neutron scattering data in Ref. [71]. Shown in the inset is the concentration dependence of the Fe magnetic moment.

$\text{NdO}_{1-x}\text{F}_x\text{FeAs}$  system was studied, it was claimed that spin ordering on Fe does not appear up to temperatures of about 2 K, where ordering of Fe and Nd spins takes place simultaneously, with the general picture of ordering similar to that shown in Fig. 10 for Fe and Ce. However, it was revealed in Ref. [74] that antiferromagnetic ordering on Fe, similar to that discussed above, in fact occurs in  $\text{NdOFeAs}$  at  $T \sim 140$  K, while difficulties with its observability are due, apparently, to the rather small value of the magnetic moment on Fe, which was found to be only  $0.25 \mu_B$ .

As to the phase diagram of 1111-systems, here some questions also remain. It was claimed in Ref. [75] that  $\mu\text{SR}$  data on  $\text{SmO}_{1-x}\text{F}_x\text{FeAs}$  suggest the existence of some narrow coexistence region of superconductivity and antiferromagnetism at doping levels in the range  $0.1 < x < 0.15$ . Naturally, a complete understanding of this situation will appear only in the course of further studies.

Neutronographic studies were also performed on different 122-compounds. Polycrystalline samples of  $\text{BaFe}_2\text{As}_2$  were studied in Ref. [76]. It was shown that a tetra-ortho

structural transition ( $I4/mmm \rightarrow Fm\bar{3}m$ ) takes place practically at the same temperature  $T_s \approx 142$  K as the antiferromagnetic transition, and spin ordering on Fe is the same as in 1111-systems, as illustrated in Fig. 11a. The magnetic moment on Fe at  $T = 5$  K is equal to  $0.87(3) \mu_B$ . Similar data were also obtained on the  $\text{SrFe}_2\text{As}_2$  single crystal [77], where structural transition at  $T_s = 220 \pm 1$  K is very sharp, indicating, in the authors' opinion, a first-order transition. At the same temperature, antiferromagnetic ordering of spins on Fe appears, which is of the same type as in  $\text{BaFe}_2\text{As}_2$  (Fig. 11a), and this transition is continuous. The magnetic moment on Fe at  $T = 10$  K is equal to  $0.94(4) \mu_B$ . These results unambiguously point to the same nature of antiferromagnetic ordering of Fe spins in two-dimensional FeAs planes in 1111- and 122-systems.

A series of single crystals of  $\text{Ba}_{1-x}\text{K}_x\text{Fe}_2\text{As}_2$  with a different  $x$  content were studied in Ref. [78] by X-ray, neutron scattering, and electrical measurement methods. As a result, the authors have produced the phase diagram shown in Fig. 11b, where a coexistence region of superconductivity

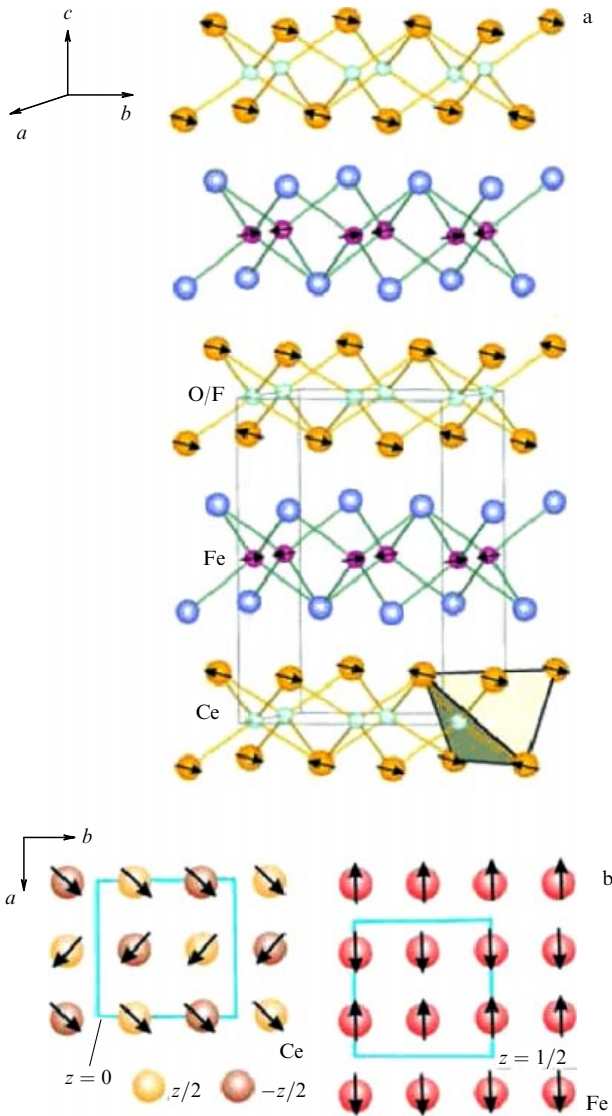


**Figure 10.** Magnetic structure of CeOFeAs: (a) general picture of spin ordering at low temperatures, and (b) magnetic elementary cells of Fe and Ce.

and antiferromagnetism is clearly seen for the interval  $0.2 < x < 0.4$ .

Concluding this section, let us highlight the recent work [79], where a neutron scattering study was performed on a  $\alpha$ -Fe(Te<sub>1-x</sub>Se<sub>x</sub>) system for the first time. It was found that in the prototype  $\alpha$ -FeTe system (with an excess of Fe), antiferromagnetic ordering of Fe spins takes place at temperatures lower than  $T_s \approx 75$  K (for Fe<sub>1.076</sub>Te) and  $T_s \approx 63$  K (for Fe<sub>1.141</sub>Te) and has the form of an incommensurate spin density wave accompanied by structural transition from the tetragonal to the orthorhombic phase ( $P4/nmm \rightarrow Pmmm$ ). The qualitative picture of spin ordering compared with the FeAs plane is displayed in Fig. 12. At the same temperature  $T_s$ , a rather sharp anomaly is also observed in the temperature dependence of electrical resistivity. For the superconducting Fe<sub>1.080(2)</sub>Te<sub>0.67(2)</sub>Se<sub>0.33(2)</sub> compound with  $T_c \approx 14$  K, spin ordering and a structural transition are absent, though well-developed fluctuations of incommensurate SDW short-range order were observed.

**2.4 Specific heat**

Specific heat measurements in new superconductors have been performed starting from the earliest works [30, 80]. As a typical example of specific heat behavior in 1111-systems, let us consider SmO<sub>1-x</sub>F<sub>x</sub>FeAs data from Ref. [80]. Shown in Fig. 13a is the temperature behavior of specific heat in this system at  $x = 0$  and  $x = 0.15$  (superconducting sample). A pronounced anomaly of specific heat is observed at  $T_s \approx 130$  K, which is obviously attributed to antiferromagnetic (SDW) (or structural tetra-ortho) transition. In the superconducting sample ( $x = 0.15$ ), this anomaly is absent. Besides this, in both samples there is a clear anomaly at  $T \approx 5$  K, which is connected with (antiferromagnetic) ordering of Sm spins. As to specific heat discontinuity at the superconducting transition, it is rather hard to resolve, and is observed, according to Ref. [80], at temperatures significantly lower than superconducting transition temperature  $T_c$  determined by zero-resistivity measurements. Apparently, this is due to the rather poor quality of samples (inhomogeneous content?).

In 122-systems, the studies of specific heat were done on single-crystal samples [81, 82]. We illustrate in Fig. 14a the

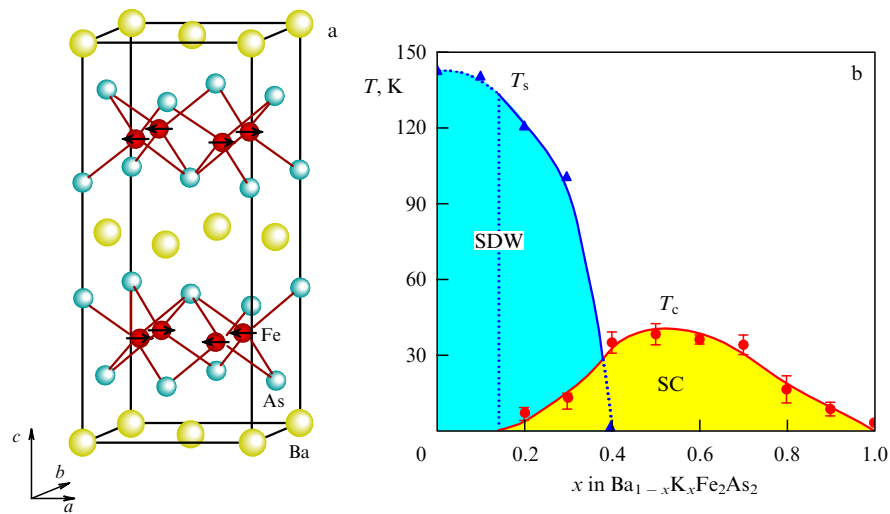


**Figure 11.** (a) Magnetic and crystal structures of BaFe<sub>2</sub>As<sub>2</sub> in an orthorhombic ( $Fmmm$ ) cell [76]. (b) Phase diagram of Ba<sub>1-x</sub>K<sub>x</sub>Fe<sub>2</sub>As<sub>2</sub> according to Ref. [78].  $T_s$  is the temperature of antiferromagnetic ordering (and structural transition), and  $T_c$  is the superconducting transition temperature.

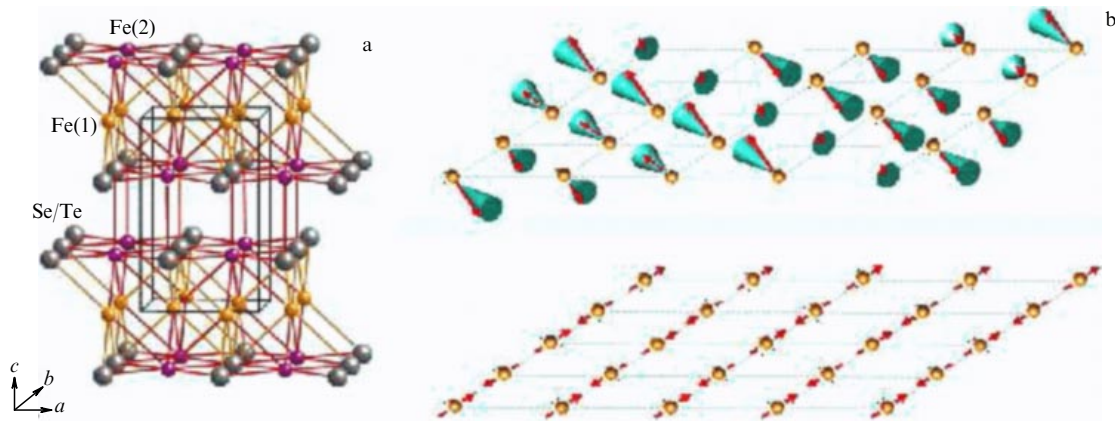


**Figure 12.** (a) Crystal structure of  $\alpha$ -FeTe/Se, with excessive iron occupying Fe(2) positions. (b) Spin ordering in  $\alpha$ -FeTe according to the data of Ref. [79], compared with antiferromagnetic ordering in the FeAs plane.

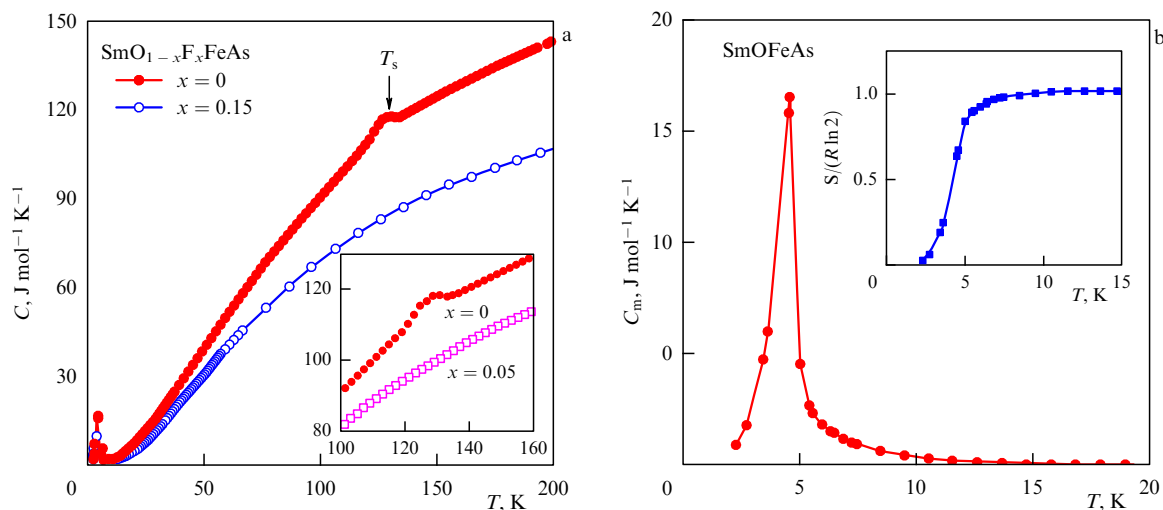


**Figure 13.** (a) Specific heat of  $\text{SmO}_{1-x}\text{F}_x\text{FeAs}$  for  $x=0$  and  $x=0.15$  (superconducting sample) [80]. Shown in the inset is the region around  $T_s = 130$  K, where (at  $x=0$ ) an anomaly is observed, usually attributed to antiferromagnetic transition of spins on Fe and absent in the superconducting sample. (b) Magnetic contribution to specific heat of  $\text{SmOFeAs}$  in the vicinity of the Sm spin ordering temperature [80]. Shown in the inset is an entropy change due to this ordering.

temperature behavior of specific heat in a superconducting single crystal of  $\text{Ba}_{0.6}\text{K}_{0.4}\text{Fe}_2\text{As}_2$  with  $T_c = 35.8$  K [82]. Detailed analysis allowed the authors to single out and study electronic specific heat coefficient  $\gamma_n$  in the normal phase, induced by a magnetic field, and in the superconducting phase. The observed dependence of  $\gamma_n$  on the magnitude of the magnetic field allowed coming to the conclusion that pairing in this system follows the s type, with a nonzero energy gap everywhere at the Fermi surface (absence of gap zeroes characteristic, e.g., of d-wave pairing in cuprates).

In Fig. 14b, a comparison is made of accurately resolved electronic specific heat discontinuity  $\Delta C_e$  at the superconducting transition with predictions of the BCS theory (weak coupling!). Agreement is quite impressive — the use of the thus determined value of  $\gamma_n \approx 63.3$   $\text{mJ mol}^{-1} \text{K}^{-2}$  gives the value of  $\Delta C_e/\gamma_n T|_{T=T_c} \approx 1.55$ , compared with the BCS theory prediction of 1.43. The fit to the BCS theoretical dependences allowed the authors to determine also the value of the energy gap at low temperatures, which was found to be  $\Delta_0 \approx 6$  meV. In Section 3.3 we shall see that this value is in good agreement with other (ARPES) available data.

## 2.5 NMR (NQR) and tunneling spectroscopy

There are already a couple of studies of peculiarities in NMR (NQR) spectra of new superconductors, pointing to certain conclusions about the possible types of superconducting pairing in these systems. In Ref. [83],  $^{75}\text{As}$  and  $^{139}\text{La}$  NMR were studied in  $\text{LaO}_{1-x}\text{F}_x\text{FeAs}$  for  $x=0, 0.04, 0.11$ . In undoped  $\text{LaOFeAs}$ , a characteristic peak (divergence) of NMR relaxation time  $1/T_1$  on  $^{139}\text{La}$  was observed at the antiferromagnetic transition temperature  $T_s \sim 142$  K, while below the NMR spectrum was too broadened, which is attributed to antiferromagnetic ordering. In a superconducting sample with  $x=0.4$  ( $T_c = 17.5$  K), the value of  $1/TT_1$  increases as temperature lowers down to  $\sim 30$  K, following the Curie–Weiss law:  $1/TT_1 \sim C/(T + \theta)$ , where  $\theta \sim 10$  K, without appearing divergence at finite temperatures, so that the occurrence of superconductivity is accompanied by the suppression of magnetic ordering. The overall picture of nuclear spin relaxation for the sample with  $x=0.11$  ( $T_c = 22.7$  K) is qualitatively different. The value of  $1/TT_1$  both on  $^{139}\text{La}$  and  $^{75}\text{As}$  nuclei decreases with lowering temperature, which is similar to the NMR picture of pseudogap behavior in underdoped cuprates, approaching a

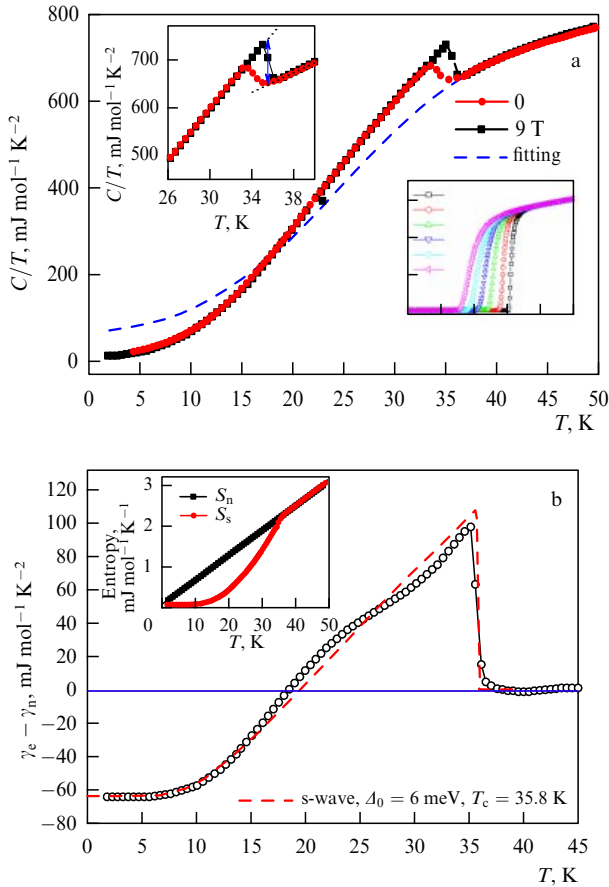


**Figure 14.** (a) Initial data on the specific heat of  $\text{Ba}_{0.6}\text{K}_{0.4}\text{Fe}_2\text{As}_2$  [82]. Shown in the insets are detailed behavior of specific heat in the vicinity of  $T_c$  and resistivity behavior in the neighborhood of the superconducting transition in different magnetic fields. (b) Electronic specific heat discontinuity and its comparison with predictions of BCS theory. Shown in the inset is the temperature behavior of entropy in the normal and superconducting states [82].

constant in the vicinity of  $T_c$ , and is well fitted by activation temperature dependence with the pseudogap value of  $\Delta_{\text{PG}} = 172 \pm 17$  K [83].

In Fig. 15a we portray the temperature dependence  $1/T_1$  on  $^{75}\text{As}$  in the  $\text{LaO}_{1-x}\text{F}_x\text{FeAs}$  system in the superconducting state ( $x = 0.04$  and  $x = 0.11$ ) and in an undoped  $\text{LaOFeAs}$  sample (on  $^{139}\text{La}$  nucleus, normalized according to  $^{139}(1/T_1)/^{75}(1/T_1) \sim 0.135$ ) [83]. It should be noted the absence of the Gebel–Slichter peak of  $1/T_1$  in the vicinity of  $T_c$ , and  $T^3$  type dependence of  $1/T_1$  in the superconducting region, characteristic of anomalous (non-s-wave!) pairing with an energy gap with zeroes at the Fermi surface, for instance, as in d-wave pairing. In fact, these dependences are well fitted using  $\Delta(\phi) = \Delta_0 \sin(2\phi)$ , where  $\phi$  is the polar angle determining the direction of the momentum in two-dimensional inverse space corresponding to the FeAs plane, with the value of  $2\Delta_0/T_c = 4.0$  [83].

Quite similar results were obtained in work [85] during the studies of NMR and NQR spectra of  $^{75}\text{As}$  nuclei in  $\text{LaO}_{1-\delta}\text{FeAs}$  ( $\delta = 0, 0.25, 0.4$ ), with  $T_c$  up to 28 K, and in  $\text{NdO}_{0.6}\text{FeAs}$  with  $T_c = 53$  K. In particular, these authors come to the conclusion that their NQR relaxation rate data for  $\text{LaO}_{0.6}\text{FeAs}$  in the superconducting phase correspond to an energy gap of the form  $\Delta = \Delta_0 \cos(2\phi)$  with  $2\Delta_0/T_c \approx 5$ , which corresponds to d-wave pairing with gap zeroes at the Fermi surface, i.e., the same pairing symmetry as in cuprates. The temperature behavior of  $1/T_1$  for  $T > T_c$ , found in this work, also gives evidence of pseudogap occurrence with the gap width  $\Delta_{\text{PG}} \approx 196$  K.

In Ref. [86],  $^{75}\text{As}$  Knight shift measurements were done in  $\text{PrO}_{0.89}\text{F}_{0.11}\text{FeAs}$ . The sharp drop in the Knight shift for  $^{75}\text{As}$  unambiguously points to the singlet nature of pairing. Details of the temperature dependence of the Knight shift were well fitted into the model with two d-wave superconducting gaps:  $\Delta = \Delta_0 \cos(2\phi)$ ,  $\Delta_0 = \alpha\Delta_1 + (1 - \alpha)\Delta_2$  with  $2\Delta_1/T_c \approx 7$  and  $2\Delta_2/T_c \approx 2.2$ ,  $\alpha = 0.4$ . In the same

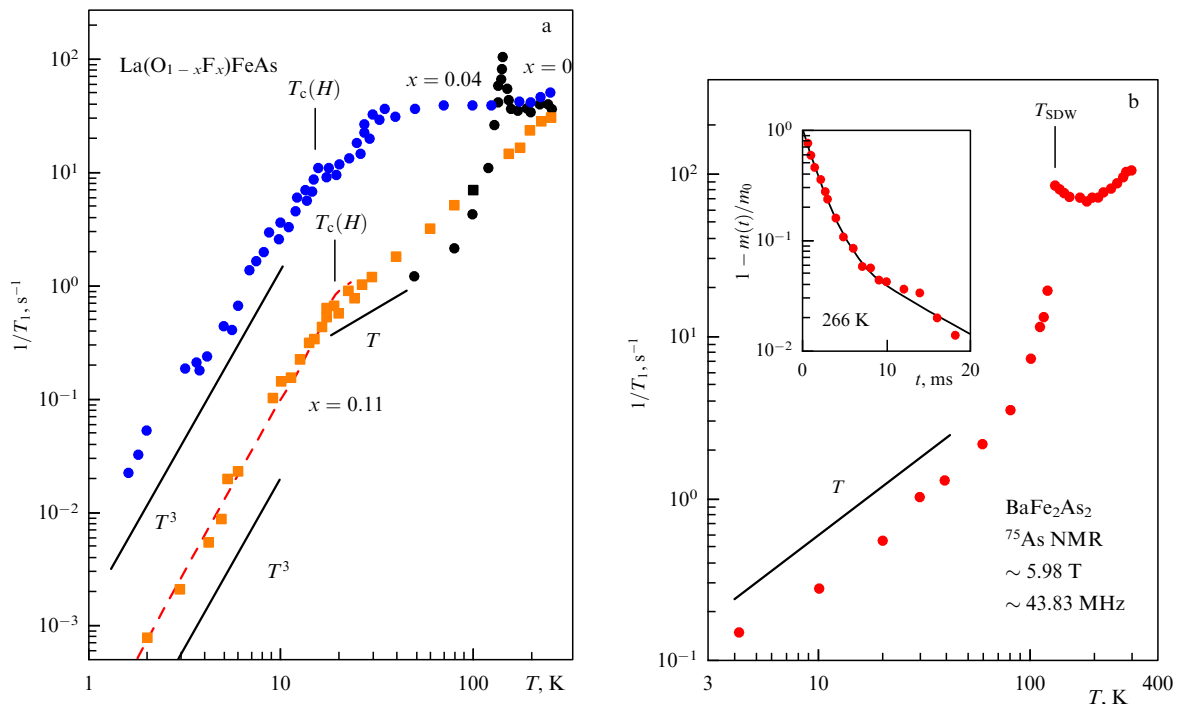


**Figure 15.** (a) Temperature dependence of NMR relaxation rate  $1/T_1$  in  $\text{LaO}_{1-x}\text{F}_x\text{FeAs}$  for  $x = 0, 0.04, 0.11$  in the low-temperature region on the order of  $T_c$  and below [83]. (b) Temperature dependence of  $1/T_1$  on  $^{75}\text{As}$  nuclei in undoped  $\text{BaFe}_2\text{As}_2$  [84].

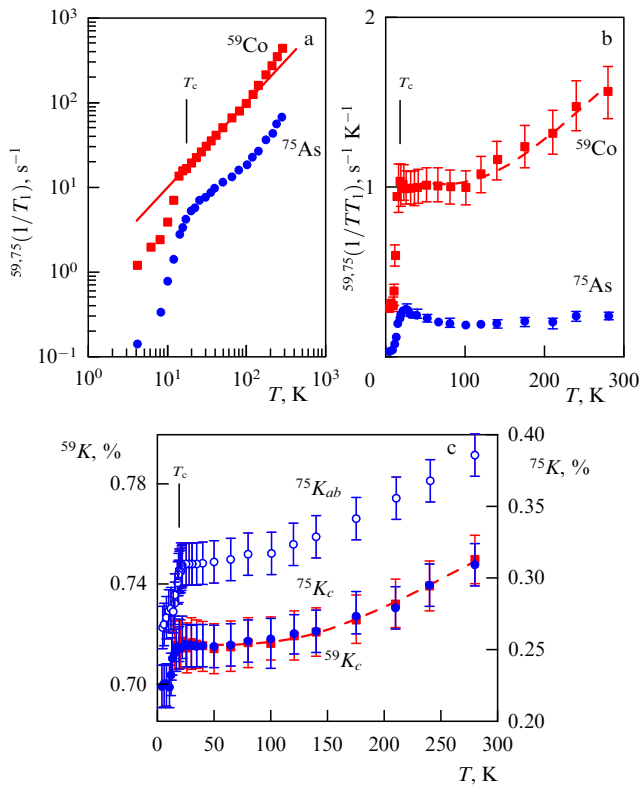


**Figure 16.** (a) Temperature dependence of  $1/T_1$  on  $^{59}\text{Co}$  and  $^{75}\text{As}$  nuclei in  $\text{BaFe}_{1.8}\text{Co}_{0.2}\text{As}_2$ , and (b) similar dependence of  $1/TT_1$ , where the dashed curve corresponds to activation dependence with pseudogap width  $\Delta_{\text{PG}} = 560 \pm 150$  K [87]. (c) Temperature dependence of the Knight shift on  $^{59}\text{Co}$  and  $^{75}\text{As}$  in the same system, where the dashed curve is described by activation dependence with the same pseudogap width.

model, the authors of Ref. [86] have successfully described the temperature dependence of  $1/T_1$  on  $^{19}\text{F}$  nuclei for  $T < T_c$ .

An NMR study of undoped  $\text{BaFe}_2\text{As}_2$  was performed in Ref. [84]. The temperature dependence of  $1/T_1$  is depicted in Fig. 15b. A clear anomaly is observed at  $T = 131$  K, which was connected by the authors to an antiferromagnetic (SDW) transition. The sharp drop in  $1/T_1$  is attributed to SDW-gap opening on part of the Fermi surface. The linear-over- $T$  behavior of the relaxation rate for  $T < 100$  K can be assigned to the relaxation of nuclear spins on conduction electrons, remaining on the ‘open’ parts of the Fermi surface. On the whole, the situation here is reminiscent of similar behavior in  $\text{LaOFeAs}$ , though there are some significant quantitative differences [84].

An NMR study of the superconducting phase in the 122-system was done on  $\text{BaFe}_{1.8}\text{Co}_{0.2}\text{As}_2$  with  $T_c = 22$  K in Ref. [87]. In Fig. 16, results on the nuclear spin relaxation rate and Knight shift are given. For temperatures below 280 K, a drop in  $1/TT_1$  is observed, which is approximated by activation dependence with (pseudo)gap width  $\Delta_{\text{PG}} \approx 560$  K (Fig. 16b). The last result is significantly larger than the pseudogap width estimates for  $\text{LaO}_{0.9}\text{F}_{0.1}\text{FeAs}$ , obtained in Ref. [83] and quoted above. Data on the Knight shift (Fig. 16c), similarly to the 1111 case, give evidence of singlet pairing. Moreover, the temperature dependence of the Knight shift above  $T_c$  also reveals pseudogap behavior with the same pseudogap width as obtained from fitting the data on the relaxation rate.

Thus, NMR data on 1111 and 122 systems are in many respects similar. Singlet pairing follows unambiguously, as

does evidence for the anomalous nature of symmetry of superconducting order parameter with probable gap zeroes at the Fermi surface (and probably the presence of two superconducting gaps). However, below we shall see that the inference about gap zeroes contradicts some other experiments and interpretations of NMR data may be quite different.

As for the  $\alpha\text{-FeSe}$  system, up to now there is only one NMR study on  $\text{FeSe}_{0.92}$  with  $T_c = 8$  K [88] (NMR on  $^{77}\text{Se}$  nuclei), demonstrating the absence of the Gebel–Slichter peak in the temperature dependence of  $1/T_1$  in the vicinity of  $T_c$  and the absence of any anomaly which can be attributed to any kind of magnetic ordering at higher temperatures, as well as the absence there of any kind of ‘pseudogap’ behavior (validity of the Korringa relation). At the same time,  $\sim T^3$ -behavior of  $1/T_1$  was observed in the  $T < T_c$  region, probably giving evidence of zeroes of the superconducting gap on the Fermi surface.

Among a number of studies using different kinds of tunneling spectroscopy, let us mention Refs [89–91]. Up to now, these experiments have been carried out on polycrystalline samples and their results are somewhat contradictory.

In Ref. [89], the method of Andreev spectroscopy was applied to  $\text{SmO}_{0.85}\text{F}_{0.15}\text{FeAs}$  with  $T_c = 42$  K. Only one superconducting gap was observed with  $2\Delta = 13.34 \pm 0.3$  meV (nearby  $T = 0$ ), which corresponds to  $2\Delta/T_c = 3.68$ , i.e., quite close to a standard BCS value of 3.52. The temperature dependence of the gap, determined in Ref. [89], also closely followed BCS theory. In the authors’ opinion, these results give evidence of the usual (s-wave) order parameter with no zeroes at the Fermi surface, in obvious contradiction to NMR findings quoted above.

A similar system,  $\text{SmO}_{0.85}\text{FeAs}$  with  $T_c = 52$  K, was studied in Ref. [90] by scanning tunneling spectroscopy at  $T = 4.2$  K. Good quality tunneling characteristics were obtained only from some parts of the sample surface, and these were fitted to the tunneling characteristics of a d-wave superconductor with  $\Delta = 8\text{--}8.5$  meV, which corresponds to  $2\Delta/T_c \sim 3.55\text{--}3.8$ .

The same method of scanning tunneling spectroscopy (microscopy) was also applied in Ref. [91] to the  $\text{NdO}_{0.86}\text{F}_{0.14}\text{FeAs}$  compound with  $T_c = 48$  K, and measurements were done at different temperatures. At temperatures significantly lower than  $T_c$ , two gaps were observed on different parts of the sample surface: the bigger one with  $\Delta \sim 18$  meV, and the smaller one with  $\Delta \sim 9$  meV. Both gaps closed at the transition point  $T = T_c$ , with the smaller gap more or less following the BCS temperature dependence. On the same parts of the surface, where the smaller gap was observed below  $T_c$ , a jumplike opening pseudogap appeared slightly above  $T_c$ , closing only at  $T = 120$  K. At present there is no reasonable interpretation of this unexpected behavior.

Notice also Ref. [92] where  $\text{SmO}_{0.9}\text{F}_{0.1}\text{FeAs}$  with  $T_c = 51.5$  K was studied by point contact spectroscopy. The authors also observed two superconducting gaps — the larger one with  $\Delta = 10.5 \pm 0.5$  meV, and the smaller one with  $\Delta = 3.7 \pm 0.4$  meV, with both gaps following BCS-like temperature dependence.

Up to now there has been no systematic tunneling data for 122-systems.

The contradictory nature of existing data measured by tunneling spectroscopy is more or less obvious. It seems likely that we have to wait for the results of experiments on single crystals.

## 2.6 Optical properties

Measurements of the optical properties of new superconductors have been done in a number of works, both on polycrystalline samples of 1111-systems [93, 94] and on single crystals of 122-systems [95, 96].

Thus, ellipsometry measurements of the dielectric permeability of the  $REO_{0.82}F_{0.18}FeAs$  ( $RE = Nd, Sm$ ) samples were made in the far infrared (IR) region [93]. It was shown that the electronic properties of these systems are strongly anisotropic (quasi-two-dimensional) and, in this sense, are analogous to those of cuprates. A noticeable suppression of optical conductivity in the superconducting state was also discovered, which was attributed by the authors to the opening of superconducting gap with  $2\Delta \approx 300 \text{ cm}^{-1}$  (37 meV), which corresponds to  $2\Delta/T_c \sim 8$ , i.e., to the strong coupling limit.

In Ref. [94], the same method was applied to studies of the dielectric permeability of  $LaO_{0.9}F_{0.1}FeAs$  with  $T_c = 27 \text{ K}$  in a wide frequency interval of 0.01–6.5 eV at temperatures ranging  $10 \leq T \leq 350 \text{ K}$ . An unusually narrow region of Drude behavior was observed, corresponding to the density of free carriers as low as  $0.040 \pm 0.005$  per unit cell, as well as signatures of pseudogap behavior at 0.65 eV. Besides that, the authors also observed a significant transfer of spectral weight to the frequency region above 4 eV. These results allowed concluding that electronic correlations [and (or) electron–phonon coupling] are very important in these systems.

Studies of reflectance and the real part of the optical conductivity in a single crystal of  $Ba_{0.55}K_{0.45}Fe_2As_2$  [95] have shown that the absorption spectrum of this system in the IR region consists of a noticeable Drude peak at low frequencies and a wide absorption band with a maximum at 0.7 eV, which the authors attributed to carrier scattering by collective (bosonic) excitations (e.g., spin fluctuations) with energies on the order of 25 meV and a strongly temperature-dependent coupling constant (with carriers).

The most convincing and interesting optical data were obtained in Ref. [96], where detailed measurements of reflectance were performed on a single crystal of  $Ba_{0.6}K_{0.4}Fe_2As_2$  with  $T_c = 37 \text{ K}$  in the infrared region and in a wide temperature interval of 10–300 K.

Figure 17 presents the data on the real part of optical conductivity  $\sigma_1(\omega)$  obtained in Ref. [96]. It is seen that close to

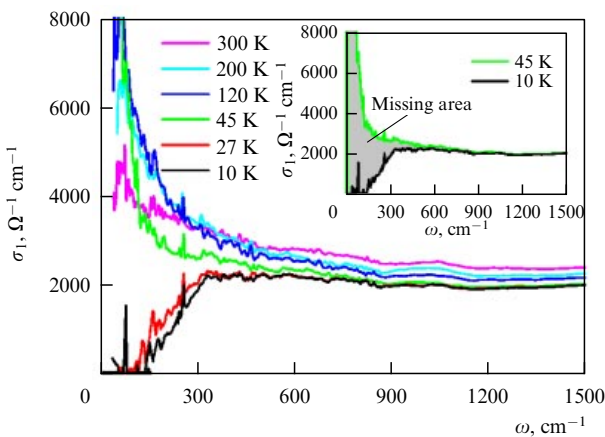


**Figure 17.** Real part of optical conductivity in  $Ba_{0.6}K_{0.4}Fe_2As_2$  at different temperatures [96]. Inset to the figure draws a comparison of the data at 10 and 45 K, where the ‘missing area’, connected with the superconducting gap opening and the formation of a condensate of Cooper pairs, is clearly seen.

and below  $T_c$  (curves, corresponding to 27 K and 10 K), a rapid drop in  $\sigma_1(\omega)$  takes place at frequencies below  $300 \text{ cm}^{-1}$ , so that conductivity is practically zero below  $150 \text{ cm}^{-1}$ , which gives evidence of a superconducting s-wave gap opening. The gap width determined by the absorption edge is  $2\Delta \approx 150 \text{ cm}^{-1}$ , which correlates well with the ARPES data to be discussed in Section 3.3.

Thus, a considerable suppression of low-frequency conductivity is observed at temperatures significantly lower than  $T_c$ , which is connected with the formation of condensate of Cooper pairs. According to the well-known Ferrell–Glover–Tinkham sum rule [97, 98], the difference in conductivities at  $T \approx T_c$  and for  $T \ll T_c$  (i.e., the so-called ‘missing area’ between appropriate curves, shown in the inset to Fig. 17) directly determines the value of condensate density:

$$\omega_{ps}^2 = 8 \int_{0^+}^{\omega_c} [\sigma_1(\omega, T \approx T_c) - \sigma_1(\omega, T \ll T_c)] d\omega, \quad (1)$$

where  $\omega_{ps}^2 = 4\pi n_s e^2 / m^*$  is the square of the plasma frequency of superconducting carriers,  $n_s$  is their density, and  $\omega_c$  is a cut-off frequency which is chosen to guarantee the convergence of  $\omega_{ps}^2$ . Then we can determine the penetration depth defined as  $\lambda = c / \omega_{ps}$ . Equation (1) yields (via the general optical sum rule) the fraction of electron (carrier) density, which is transferred to the  $\delta(\omega)$  singularity of  $\sigma_1(\omega)$ , corresponding to the superconducting response of the condensate. A direct estimate of the missing area gives for the penetration depth  $\lambda$  the value equal to 2080 Å, which agrees well with other data [96].

## 2.7 Phonons and spin excitations: neutron spectroscopy

Up to now, a number of experiments have already been carried out to study collective excitations, i.e., phonons and spin waves, in new superconductors, which is of principal importance for the clarification of the nature of Cooper pairing in these systems. Below we shall mainly deal with experiments on inelastic neutron scattering.

In Ref. [99], inelastic neutron scattering was studied in the  $LaO_{0.87}F_{0.13}FeAs$  compound with  $T_c \approx 26 \text{ K}$ . Characteristic maxima of phonon density of states were observed at 12 and 17 meV.

The phonon density of states in  $LaO_{1-x}F_xFeAs$  (for  $x = 0$  and  $x \sim 0.1$ ) was studied in more detail in Ref. [100], where it was also compared with the results of phonon spectrum calculations done in Ref. [101]. The main findings of this work are given in Fig. 18a–c, where we can see both the general structure of the phonon density of states and satisfactory agreement with the available calculations [101]. It is also evident that the phonon spectrum of a prototype 1111-system differs very little from that observed in a doped (superconducting) sample. The origin of the peaks in the phonon density of states is well explained on the basis of theoretical calculations.

The phonon density of states in 1111-systems was also studied by nuclear resonance inelastic synchrotron radiation scattering [103] (in La-based systems) and by inelastic X-ray scattering [104] (in La- and Pr-based systems). In all cases, the results are quite similar to those obtained by inelastic neutron scattering and are in satisfactory agreement with theoretical calculations.

As for 122-systems, up to now there has been work on inelastic neutron scattering in the prototype  $BaFe_2As_2$  system

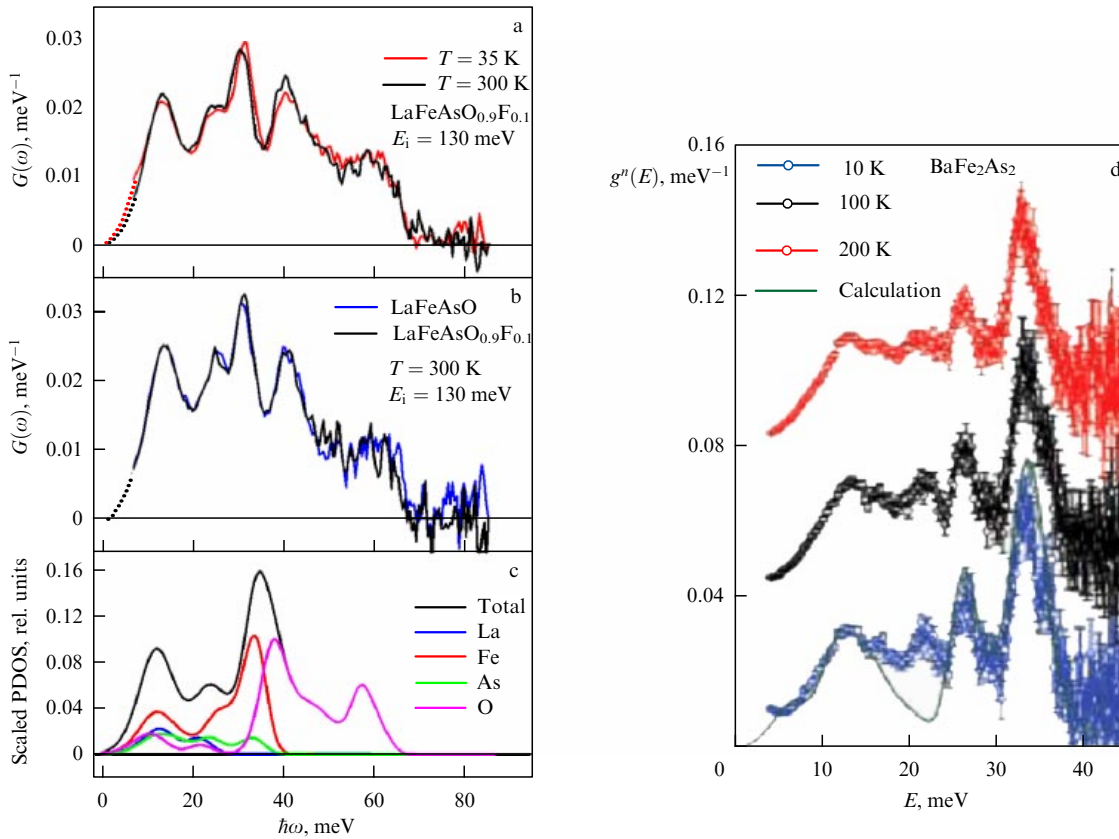


**Figure 18.** Phonon density of states in  $\text{LaO}_{1-x}\text{F}_x\text{FeAs}$ , obtained from inelastic neutron scattering (a, b) [100] and compared with calculations (c) in Ref. [101]. (d) Comparison of experimental and calculated phonon density of states in  $\text{BaFe}_2\text{As}_2$  [102].

[102, 105], where consistent results have been obtained, which are also in agreement with the calculated results for the phonon spectrum, obtained in these works. As an example, we compare in Fig. 18d calculated and experimental phonon densities of states for this system, which were found in Ref. [102]. From this figure we see quite satisfactory agreement, except for an additional peak at a frequency on the order of 21.5 meV, observed in the experiments.

The dynamics of spin excitations in new superconductors were studied by neutronography in  $\text{SrFe}_2\text{As}_2$  [106] and  $\text{BaFe}_2\text{As}_2$  [107], i.e., in undoped samples, where antiferromagnetic ordering takes place at low temperatures.

In particular, it was shown in Ref. [106] that the spectrum of magnetic excitations is characterized by a gap of width  $\Delta \leq 6.5 \text{ meV}$ , while above this gap well-defined spin waves are observed, and the measurement of their velocity allowed estimating exchange integrals (in the localized spin model). In the vicinity of the temperature of antiferromagnetic transition, no signs of critical scattering were observed, which in the opinion of the authors implies that the magnetic transition here is of the first order [106].

Qualitatively similar results (though without detailed measurements of spin wave dispersion) were obtained in Ref. [107], where it was shown that the magnon spectrum continues up to energies which are significantly higher than typical phonon frequencies ( $\sim 40 \text{ meV}$ ) and ends at energies of about 170 meV.

## 2.8 Other experiments

In our rather concise review of experiments on studying new superconductors we could not pay attention to a number of

important investigations; a more detailed discussion of experiments on critical magnetic fields (in particular, measurements of  $H_{c1}$ ), direct measurements of penetration depth, and experiments on X-ray photoemission remained outside our presentation. We have practically paid no attention to experiments on traditional transport properties in the normal state (such as the Hall effect and thermoelectricity). This is connected mainly with the limited size of this review, as well as with the personal preferences of the author. In Section 3.3 comprising the theoretical part of this review, we shall return to the discussion of a number of extra experiments. In particular, we shall pay great attention to experiments with angle-resolved photoemission (ARPES), which are more appropriately considered in parallel with discussions of the electronic spectrum of these systems. The same applies to some other experiments on the determination of Fermi surfaces (quantum oscillation effects in strong magnetic fields).

## 3. Electronic spectrum and magnetism

### 3.1 Band structure (LDA)

Clarification of the structure of the electronic spectrum of new superconductors is crucial for explaining their physical properties. Accordingly, since the first days, different teams have started detailed band-structure calculations for all classes of these compounds, based primarily on different realizations of the general local density approximation (LDA) approach.

The first calculations of the electronic spectrum of iron oxypnictide LaOFeP were performed in Ref. [108], yet before the discovery of high-temperature superconductivity in FeAs-based systems. For LaOFeAs, such calculations were done almost simultaneously in Refs [101, 109–111]. In the following, similar calculations were also performed for other 1111-systems, as well as for 122-systems [112, 113], 1111-systems [113–115], and  $\alpha$ -FeSe [116]. As the results obtained in all these works were more or less similar, we shall concentrate below in more detail on our group works [117–120], referring to publications of other authors where necessary. We shall also limit ourselves mainly to the results obtained for the nonmagnetic tetragonal phase of 1111 and 122 systems (as well as 111), as superconductivity is realized just in this phase.

In Ref. [117] we have performed *ab initio* calculations of the electronic structure for a number of oxypnictides from the series  $REO_{1-x}F_xFeAs$  [where  $RE = La, Ce, Nd, Pr, Sm$ , and also for the hypothetical (at that time) case of  $RE = Y$ ] in the framework of the standard LDA – LMTO approach [121].

In Fig. 19a we made a comparison of electronic spectra of the LaOFeAs and PrOFeAs compounds [117] in the main symmetry directions in the Brillouin zone. It can be seen that differences in the spectra related to the replacement of the rare-earth ion (as well as a small change in lattice constants) are rather small. In a narrow enough energy interval (on the order of  $\pm 0.2$  eV) close to the Fermi energy, which is relevant to superconductivity, these spectra practically coincide.

This is also clearly seen from a comparison of the densities of states shown in Fig. 19b. In fact, the densities of states of both compounds close to the Fermi level are just the same (up to a few percent). This is typical also for other compounds from the rare-earth series  $REO_{1-x}F_xFeAs$  [117].

The only noticeable difference in the spectra of these systems with different rare-earth ions manifests itself in the growth of tetrahedral splitting due to lattice compression, which appears at energies on the order of  $-1.5$  eV for d-states of Fe, and  $-3$  eV for p-states of As.

From a comparison of partial densities of states we can also see that the value of the density of states close to the Fermi level is determined almost entirely by d-states of Fe (with a very insignificant contribution from p-states of As). In this sense, we can say that all phenomena related to superconductivity in these compounds take place in the square lattice of Fe within the FeAs layer.

Naturally, most of these peculiarities of electronic spectra may be attributed to the quasi-two-dimensional character of the compounds under study. For example, the insensitivity of electronic spectra to the type of a rare-earth ion is simply due to the fact that electronic states of *REO* layers are far from the Fermi level, and p-states of O only weakly overlap with the d-states of Fe and p-states of As in FeAs layers. Accordingly, hybridization of the d-states of Fe and p-states of As is more significant, but still not very strong, as demonstrated by band structure calculations.

Thus, the situation with rare-earth substitutions in the *REOFeAs* series seems to be largely analogous to the similar one in cuprates like  $REBa_2Cu_3O_{7-x}$ , which were studied in the early days of HTSC research [72, 122]. In these compounds, the electronic states of rare-earth ions do not overlap with the electronic states in conducting  $CuO_2$  planes either, which leads to the well-known fact of the almost complete independence of superconducting  $T_c \sim 92$  K on the type of rare earth in the series  $RE = Y, Nd, Sm, Eu, Gd,$

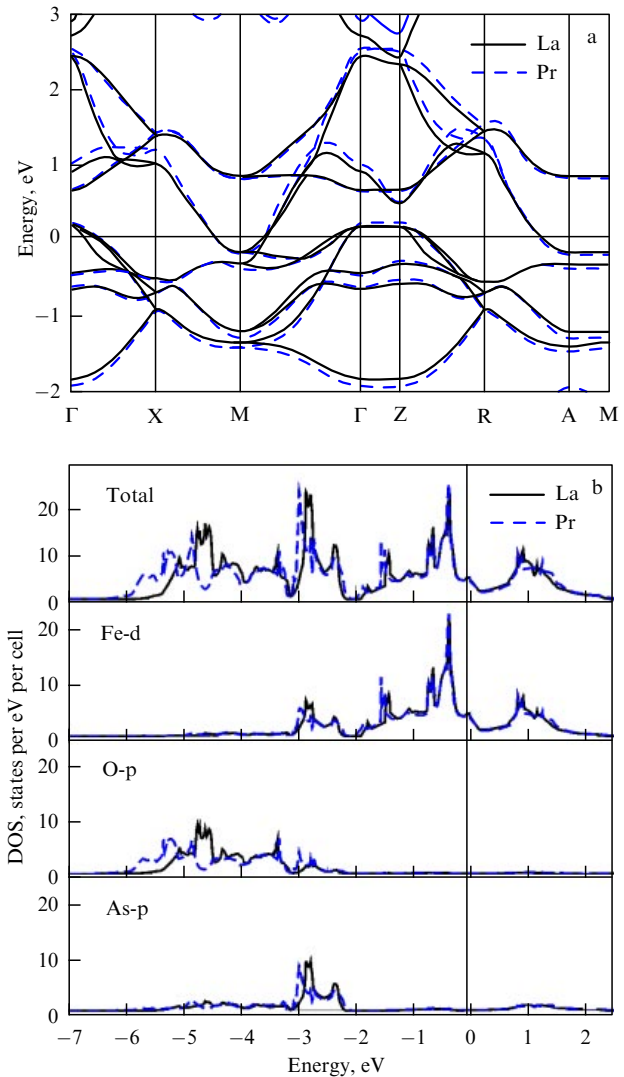


**Figure 19.** (a) Electronic spectra of LaOFeAs and PrOFeAs in high-symmetry directions in the Brillouin zone of a tetragonal lattice, obtained within the LDA approach [117]. (b) Comparison of the total and partial densities of states in LaOFeAs and PrOFeAs [117].

Ho, Er, Tm, Yb, Lu, Dy [124], with only two exceptions relating to a much lower  $T_c \sim 60$  K in the case of La and the complete absence of superconductivity in the case of a Pr-based compound [72].

Similarly, the almost identical electronic structure of iron oxypnictides like *REOFeAs* with different *RE* in a wide enough energy interval around the Fermi level seems to lead inevitably to approximately the same values of superconducting transition temperature  $T_c$  (for any BCS-like microscopic mechanism of pairing). Different rare-earth ions just do not influence electronic structure, at least in this energy interval around the Fermi level, and, accordingly, do not change the value of the pairing coupling constant. Also, there is no special reasons to believe that the replacement of rare-earth ion will change the phonon spectrum of these systems much, or the spectrum of magnetic excitations in the FeAs layer.

Thus, it would seem that we have a kind of rare-earth puzzle — in contrast to cuprate series  $REBa_2Cu_3O_{7-x}$ , different rare-earth substitutions in the *REOFeAs* series lead to a rather wide scatter in  $T_c$  values, from  $\sim 26$  K in the case of La-based system to  $\sim 55$  K in the case of Nd and Sm. At the

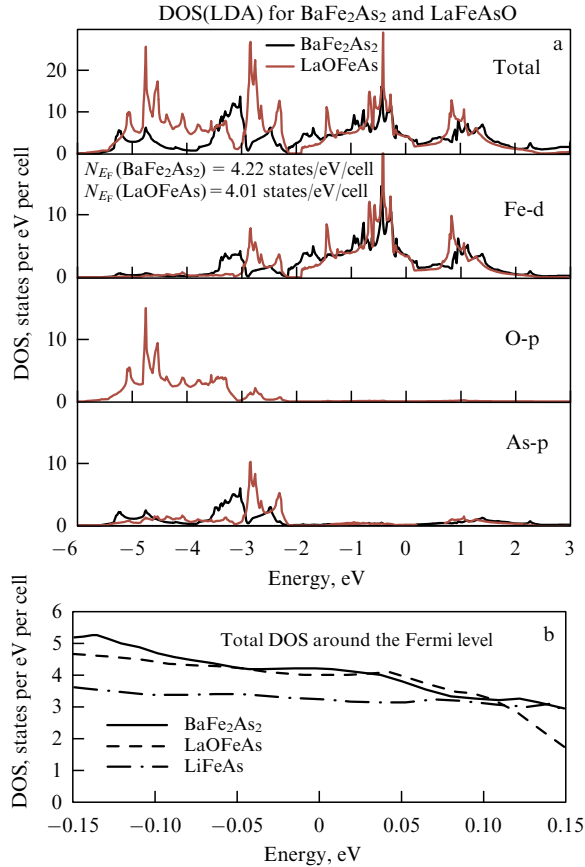


**Figure 20.** (a) Comparison of the total electronic density of states and partial densities of states in LaOFeAs and BaFe<sub>2</sub>As<sub>2</sub> [118]. (b) Comparison of densities of states in a narrow energy interval around the Fermi level in LaOFeAs, BaFe<sub>2</sub>As<sub>2</sub>, and LiFeAs [119].

moment, we can propose two possible explanations of this puzzle:

(1) Different qualities of samples (disorder effects) can lead to a rather wide scatter in  $T_c$  values, because internal disorder can strongly influence the value of critical temperature, especially for anomalous pairings (anisotropic s-wave, even more so p- or d-wave pairing, triplet pairing, etc.), which are widely being discussed at present for FeAs superconductors [110, 123]. This possibility is qualitatively analogous to the case of copper oxides, where d-wave pairing is realized, which is strongly suppressed by disorder. This argumentation was used, for example, to explain typically lower values of  $T_c$  in LaBa<sub>2</sub>Cu<sub>3</sub>O<sub>7-x</sub>, which were attributed to disorder in the positions of La and Ba ions, as well as to oxygen vacancies [72]. In fact, this point of view is confirmed by reports on the synthesis of LaO<sub>1-x</sub>FeAs with  $T_c \sim 41$  K [34], as well as by the synthesis of the initially hypothetical [117] YO<sub>1-x</sub>FeAs system, first with  $T_c \sim 10$  K [124] and later (synthesis under high pressure) with  $T_c \sim 46$  K [125]. In this last paper, 1111-compounds based on Ho, Dy, and Tb were also synthesized, leading to  $T_c$  values on the order of 50, 52, and 48 K, respectively. It seems quite probable that the best prepared samples of the 1111 series may achieve values of  $T_c \sim 55$  K, as obtained in the most ‘favorable’ cases of Sm and Nd. This stresses the necessity of systematic studies of disorder effects in new superconductors.

(2) However, we cannot exclude also the other physical reasons for  $T_c$  variability in the REOFeAs series, connected, for instance, with spin ordering on rare-earth ions (like Ce, Pr,

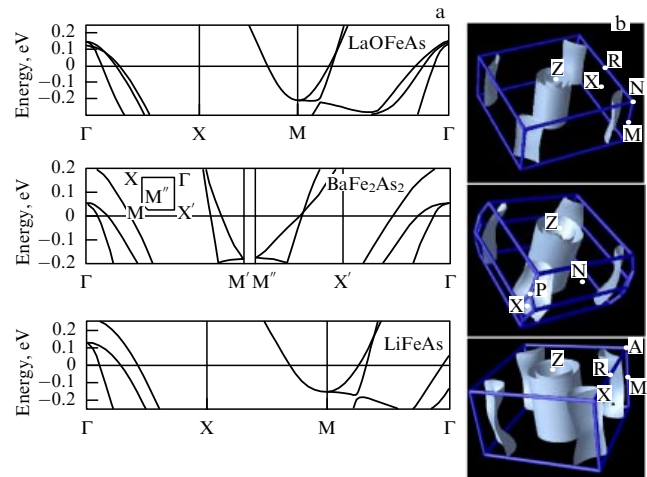


**Figure 21.** (a) Electronic spectra of LaO<sub>1-x</sub>F<sub>x</sub>FeAs, BaFe<sub>2</sub>As<sub>2</sub>, and LiFeAs in a narrow interval of energies close to the Fermi level, relevant to the formation of the superconducting state. (b) Fermi surfaces of these compounds [117, 119].

Nd, Sm, Gd, which possess magnetic moments). Above, we have already mentioned the unusually high coupling of these moments with moments on Fe. Moreover, the temperature of rare-earth moments ordering is known experimentally to be an order of magnitude higher than in the REBa<sub>2</sub>Cu<sub>3</sub>O<sub>7-x</sub> systems [72], which also points to rather strong magnetic couplings. The latter may significantly influence, for example, the spin fluctuation spectrum in FeAs layers (and  $T_c$  values in the case of the magnetic mechanisms of pairing [110, 123]).

In Fig. 20a we made a comparison of the total electronic density of states and partial densities of states in the LaOFeAs and BaFe<sub>2</sub>As<sub>2</sub> samples [118]. It is seen that again we have almost the same values of DOSs in an energy interval around the Fermi level, relevant to superconductivity. We can see it in more detail in Fig. 20b, where densities of states are compared in a narrow ( $\pm 0.15$  eV) energy interval close to the Fermi level in LaOFeAs, BaFe<sub>2</sub>As<sub>2</sub>, and LiFeAs [119]. The densities of states in this energy interval are almost energy independent (quasi-two-dimensionality!) and only slightly different (though, in principle, one can notice some correlation of these values of DOS at the Fermi level and the values of  $T_c$  in these compounds).

The bandwidth of d-states of Fe in BaFe<sub>2</sub>As<sub>2</sub> is approximately 0.3 eV larger than in LaOFeAs, which may be connected with shorter Fe–As bonds, i.e., with larger Fe-d–As-p hybridization. In both compounds, bands crossing the Fermi level are formed mainly from three d-orbitals of Fe with  $t_{2g}$  symmetry, namely  $xz$ ,  $yz$ ,  $xy$ . A similar situation is also realized for LiFeAs.

In Fig. 21a we exhibit electronic dispersions in high-symmetry directions in all three main classes (1111, 122, and 111) of new superconductors in a narrow ( $\pm 0.2$  eV) energy interval around the Fermi level, where the superconducting state is formed [118, 119]. It can be seen that electronic spectra of all systems in this energy interval are very close to each other. In the general case, the Fermi level is crossed by five bands formed by d-states of Fe. Of these, three form hole-like Fermi surface pockets close to the  $\Gamma$  point, and the others form two-electron-like pockets at the corners of the Brillouin zone (note that the Brillouin zones of 1111, 111, and 122 systems are slightly different due to existing differences in lattice symmetry).

It is not difficult to understand that this kind of a band structure leads to similar Fermi surfaces of these compounds — appropriate calculated results are given on the right-hand side of Fig. 21b: there are three hole-like cylinders at the center of the Brillouin zone and two electron-like ones at the corners. The almost cylindrical form of the Fermi surfaces reflects the quasi-two-dimensional nature of the electronic spectra in new superconductors. The smallest of the hole-like cylinders is usually neglected in the analysis of superconducting pairings, as its contribution to electronic properties is rather small (the smallness of its phase space volume). At the same time, from the general picture of the electronic spectrum it is clear that superconductivity is formed in a multiple band system with several Fermi surfaces of different (electron or hole-like) natures, which is drastically different from the simple one-band situation in HTSC cuprates. In Section 3.3 we shall see that the results of LDA calculations of an electronic structure correlate rather well with ARPES experiments.

LDA calculations of the band structure of  $\alpha$ -FeSe were performed in a recent paper [116]. Dropping the details, it should be noted that the results are qualitatively quite similar to those described above for 1111, 122, and 111 systems. In particular, the form of Fermi surfaces is qualitatively the same, while conduction bands near the Fermi level are formed from d-states of Fe.

The first calculations of the band structure of the Sa(Ca)FFeAs compounds were done in Refs [120, 126]. Naturally enough, the band structure and Fermi surfaces in these compounds are also very similar to those obtained earlier for REOFeAs systems. The only disparity lies in a slightly more pronounced quasi-two-dimensional nature of the electronic spectra in these compounds.

### 3.2 ‘Minimal’ model

The relative simplicity of the electronic spectrum of FeAs superconductors in the neighborhood of the Fermi level (see Fig. 21) suggests a possibility to formulate a kind of ‘minimal’ analytic or semianalytic model of the spectrum (e.g., in the tight-binding approximation), which will provide a semi-quantitative description of electrons in the vicinity of the Fermi level, being sufficient for a theoretical description of the superconducting state and magnetic properties of FeAs planes. Up to now, several variants of such a model have already been proposed [127–130]. Below, we shall limit ourselves to a brief description of the simplest (and crudest) variant of this model, proposed by Scalapino and coworkers (see Ref. [127]).

The schematic structure of a single FeAs layer is displayed in Fig. 22a. Fe ions form a square lattice surrounded by layers of As ions which also form a square lattice and reside at the centers of squares of Fe ions and are displaced upwards or downwards with respect to the Fe lattice in a checkerboard manner, as illustrated in Fig. 22a. This leads to two inequivalent positions of Fe, so that there are two ions of Fe and two As ions in an elementary cell. The LDA calculations described in Section 3.1 imply that the main contribution to the electronic density of states in a wide enough energy interval around the Fermi level is due to the d-states of Fe. Thus, we can consider the simplified model which primarily takes into account three orbitals of Fe, namely  $d_{xz}$ ,  $d_{yz}$ , and  $d_{xy}$  (or  $d_{x^2-y^2}$ , which is just the same). As a further simplification, the role of  $d_{xy}$  (or  $d_{x^2-y^2}$ ) orbitals can be effectively taken into account by introducing transfer inte-

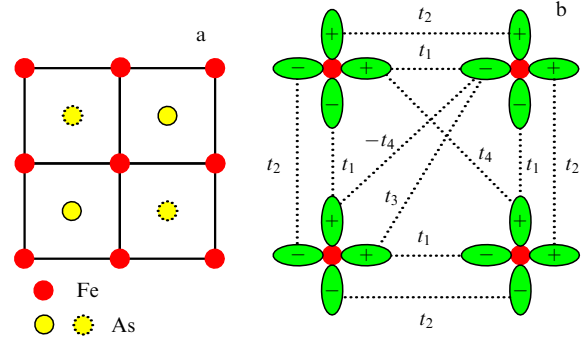


**Figure 22.** (a) Fe ions in an FeAs layer form a quadratic lattice containing two Fe ions and two As ions in an elementary cell. As ions are placed above (solid dots) or under (dashed circles) centers of the squares formed by Fe. (b) Transfer integrals taken into account in the two-orbital ( $d_{xz}, d_{yz}$ ) model on the square lattice of Fe. Here,  $t_1$  is the transfer integral between nearest  $\sigma$ -orbitals, and  $t_2$  is the transfer integral between nearest  $\pi$ -orbitals. Also taken into account are transfer integrals  $t_4$  between different orbitals, and  $t_3$  between identical orbitals on the second nearest neighbors. Also shown are projections of  $d_{xz}, d_{yz}$  orbitals onto the  $xy$  plane [127].

grals between  $d_{xz}, d_{yz}$  orbitals on the second nearest neighbors. Accordingly, we may consider a square lattice with two degenerate ‘ $d_{xz}, d_{yz}$ ’ orbitals at each site, with the transfer integrals shown in Fig. 22b. As we shall see below, such a model produces a picture of two-dimensional Fermi surfaces in the FeAs layer, which is in qualitative agreement with LDA results.

For an analytical description of this model it is convenient to introduce a two-component spinor

$$\psi_{\mathbf{k}s} = \begin{pmatrix} d_{xs}(\mathbf{k}) \\ d_{ys}(\mathbf{k}) \end{pmatrix}, \quad (2)$$

where  $d_{xs}(\mathbf{k})$  ( $d_{ys}(\mathbf{k})$ ) annihilates the  $d_{xz}$  ( $d_{yz}$ ) electron with spin  $s$  and wave vector  $\mathbf{k}$ . A tight-binding Hamiltonian can be written out as

$$H_0 = \sum_{\mathbf{k}s} \psi_{\mathbf{k}s}^\dagger [(\varepsilon_+(\mathbf{k}) - \mu) \hat{1} + \varepsilon_-(\mathbf{k}) \hat{\tau}_3 + \varepsilon_{xy}(\mathbf{k}) \hat{\tau}_1] \psi_{\mathbf{k}s}, \quad (3)$$

where  $\hat{\tau}_i$  are the Pauli matrices, and

$$\begin{aligned} \varepsilon_{\pm}(\mathbf{k}) &= \frac{\varepsilon_x(\mathbf{k}) \pm \varepsilon_y(\mathbf{k})}{2}, \\ \varepsilon_x(\mathbf{k}) &= -2t_1 \cos k_x a - 2t_2 \cos k_y a - 4t_3 \cos k_x a \cos k_y a, \\ \varepsilon_y(\mathbf{k}) &= -2t_2 \cos k_x a - 2t_1 \cos k_y a - 4t_3 \cos k_x a \cos k_y a, \\ \varepsilon_{xy}(\mathbf{k}) &= -4t_4 \sin k_x a \sin k_y a. \end{aligned}$$

Finally, the single-particle Green’s function in the Matsubara representation takes the following form

$$\hat{G}_s(\mathbf{k}, i\omega_n) = \frac{(i\omega_n - \varepsilon_+(\mathbf{k})) \hat{1} - \varepsilon_-(\mathbf{k}) \hat{\tau}_3 - \varepsilon_{xy}(\mathbf{k}) \hat{\tau}_1}{(i\omega_n - E_+(\mathbf{k}))(i\omega_n - E_-(\mathbf{k}))}, \quad (4)$$

where

$$E_{\pm}(\mathbf{k}) = \varepsilon_{\pm}(\mathbf{k}) \pm \sqrt{\varepsilon_+^2(\mathbf{k}) + \varepsilon_{xy}^2(\mathbf{k})} - \mu. \quad (5)$$

In Fig. 23a we displayed the appropriate electronic spectrum for the following values of transfer integrals:  $t_1 = -1$ ,  $t_2 = 1.3$ , and  $t_3 = t_4 = -0.85$  (in units of  $|t_1|$ ).

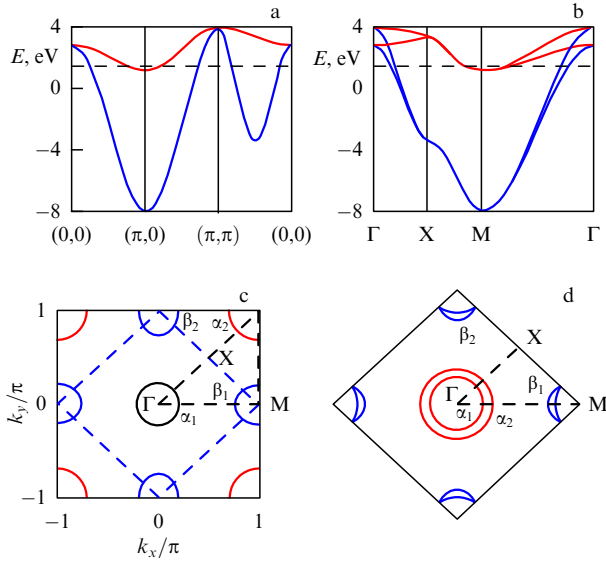


**Figure 23.** (a) Electronic spectrum in the two-orbital model with transfer integrals  $t_1 = -1$ ,  $t_2 = 1.3$ ,  $t_3 = t_4 = -0.85$  (in units of  $|t_1|$ ) and chemical potential  $\mu = 1.45$ , taken along directions  $(0,0) \rightarrow (\pi/a,0) \rightarrow (\pi/a,\pi/a) \rightarrow (0,0)$ . (b) The same spectrum in a twice downfolded Brillouin zone, with an appropriate redefinition of the  $\Gamma$ , X, M points. (c) The Fermi surface in the two-orbital model in the Brillouin zone corresponding to one Fe ion per elementary cell;  $\alpha_{1,2}$  — hole-like Fermi surfaces defined by  $E_-(k_F) = 0$ , and  $\beta_{1,2}$  — electron-like Fermi surfaces defined by  $E_+(k_F) = 0$ . Dashed lines show the Brillouin zone for two Fe ions in an elementary cell. (d) Fermi surfaces in the downfolded Brillouin zone corresponding to two Fe ions in an elementary cell [127].

Let us now take into account the fact, mentioned above, that in a real FeAs layer there are two Fe ions per elementary cell. Accordingly, the Brillouin zone is twice as small and the spectrum must be folded down into this new zone, as shown in Fig. 23b. In Fig. 23c, d we depicted Fermi surfaces which are obtained in this simplified model of the electronic spectrum. In the large Brillouin zone corresponding to the lattice with one Fe ion per elementary cell there are two hole-like pockets, denoted as  $\alpha_1$  and  $\alpha_2$ , which are defined by the equation  $E_-(k_F) = 0$ , and two electron-like pockets  $\beta_1$  and  $\beta_2$ , defined by  $E_+(k_F) = 0$ . To compare them with the results of band structure calculations (LDA), these Fermi surfaces should be folded down into a Brillouin zone that is half as big, corresponding to two Fe ions in an elementary cell of the crystal and being shown by dashed lines in Fig. 23c. The result of such downfolding is given in Fig. 23d. It is evident that the Fermi surfaces obtained in this way are in qualitative agreement with the results of LDA calculations (only the third, less relevant, small hole-like pocket at the zone center is absent). Despite its crudeness, this model of the spectrum, proposed in Ref. [127], is quite appropriate for qualitative analysis of the electronic properties of FeAs-based superconductors.

### 3.3 Angle-resolved photoemission spectroscopy (ARPES)

At the moment there are already a number of papers where the electronic spectrum and Fermi surfaces in new superconductors were studied using angle-resolved photoemission spectroscopy [131–141], a reliable method which proved its effectiveness in HTSC cuprates [13, 142] due, by the way, to the quasi-two-dimensional nature of the electronic spectrum in these systems. In fact, ARPES studies for FeAs-based superconductors immediately provided valuable informa-

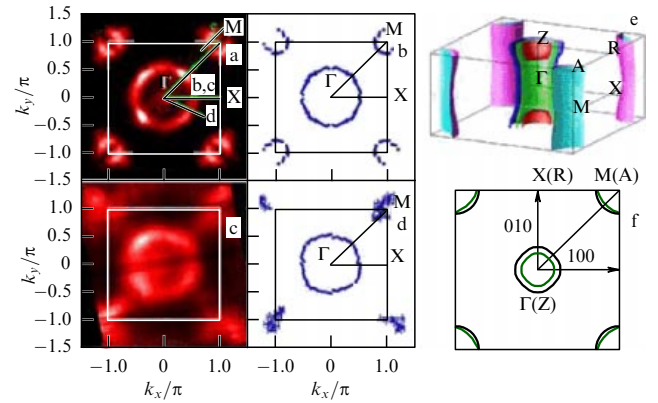


**Figure 24.** (a) ARPES intensity map, and (b) Fermi surfaces determined for  $\text{NdO}_{0.9}\text{F}_{0.1}\text{FeAs}$  at a photon energy of 22 eV and  $T = 70$  K. (c, d) The same as in figures a, b, but for a photon energy of 77 eV [131]. (e, f) Three-dimensional and two-dimensional pictures of Fermi surfaces in  $\text{NdOFeAs}$ , obtained from LDA calculations [131].

tion clarifying the general form of their spectrum, Fermi surfaces, and widths and peculiarities of superconducting gaps. It should be noted that for 1111-systems there has so far been only one ARPES work [131], which is due to the absence of good single crystals, so that all the remaining studies were performed on single crystals of 122-systems. Below we shall discuss the results of some of these papers in more details.

ARPES measurements in Ref. [131] were performed on micron-sized single crystals (on the order of  $200 \times 200 \times 30 \mu\text{m}$ , with  $T_c \sim 53$  K). In Fig. 24 we exhibited ARPES intensity maps (which are proportional to spectral density) in the  $\text{NdO}_{0.9}\text{F}_{0.1}\text{FeAs}$  system, allowing us to determine the form of Fermi surfaces in the two-dimensional Brillouin zone corresponding to FeAs planes. It can be seen that the general qualitative picture is in reasonable agreement with the results of LDA calculations of the band structure, though only one hole-like cylinder is resolved around the  $\Gamma$  point, and electron-like cylinders at the corners (point M) are resolved rather poorly. The width of the superconducting gap on the hole-like cylinder, estimated from ARPES spectra, was determined to be on the order of 20 meV [132], corresponding to  $2\Delta/T_c \sim 8$ .

In Ref. [134], ARPES measurements were carried out for a single crystal of superconducting  $(\text{Sr}, \text{K})\text{Fe}_2\text{As}_2$  with  $T_c = 21$  K. The ARPES map of the Fermi surfaces obtained is displayed in Fig. 25. In contrast to other works, here the authors succeeded in resolving all three hole-like cylinders around the point  $\Gamma$ , in complete agreement with the majority of LDA calculations of the spectrum. Resolution at the corners of the Brillouin zone (point M) turned out to be much poorer, so that the topology of the electronic sheets of the Fermi surface remained unclear.

Shown in Fig. 26 are the energy bands in high-symmetry directions of the Brillouin zone, obtained from ARPES measurements [134]. On the one hand, these data correlate well with the results of the band structure calculations in work [118], taking into account the Fermi level shift in energy downwards by  $\sim 0.2$  eV (in complete accordance with the hole doping of the superconducting sample). On the other hand, rather significant band narrowing in comparison with LDA results is also observed, which can be attributed to strong electronic correlations (cf. below).

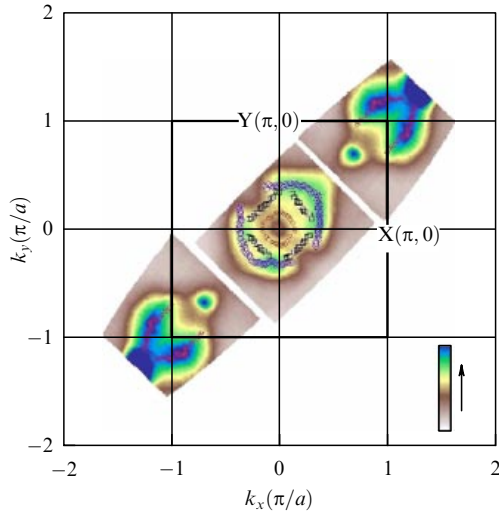


**Figure 25.** ARPES map of the Fermi surfaces in  $(\text{Sr, K})\text{Fe}_2\text{As}_2$  [134].

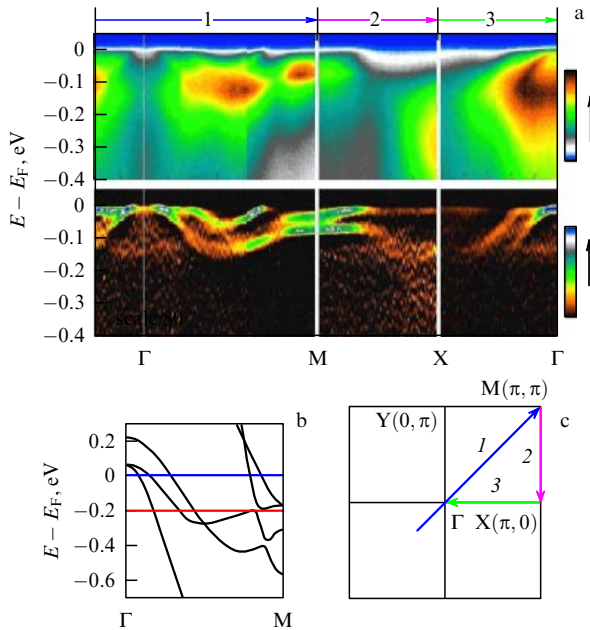


**Figure 26.** (a) Energy bands determined from ARPES data on  $(\text{Sr, K})\text{Fe}_2\text{As}_2$  [134]; in the upper part of the figure — initial ARPES intensity data, below — their second derivative, allowing following dispersion curves. (b) Band spectrum obtained in Ref. [118]. (c) Directions in the Brillouin zone, along which measurements have been made.

In Ref. [136] for the first time Fermi surfaces of  $\text{Ba}_{0.6}\text{K}_{0.4}\text{Fe}_2\text{As}_2$  ( $T_c = 37$  K) were studied in detail,<sup>4</sup> while ARPES measurements of superconducting gaps (and their temperature dependence) on different sheets of the Fermi surface were made. Schematically, the results of these measurements are given in Fig. 27. Two superconducting gaps were discovered — a large one ( $\Delta \sim 12$  meV) on a small hole-like cylinder around point  $\Gamma$  and on the electron-like cylinders around point M, and a small one ( $\Delta \sim 6$  meV) on a big hole-like cylinder around point  $\Gamma$ . Both gaps close at the same temperature coinciding with  $T_c$ , have no zeroes, and are

<sup>4</sup> A small third hole-like cylinder around point  $\Gamma$  was not observed, probably due to insufficient resolution of ARPES spectra.

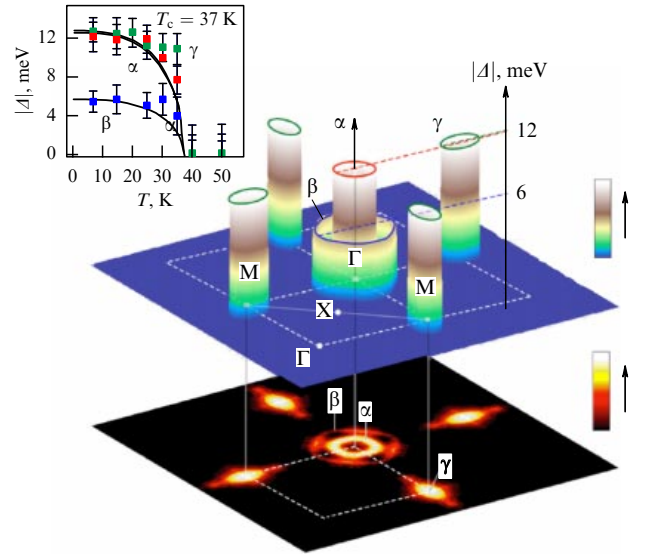


**Figure 27.** Schematic three-dimensional picture of the superconducting gap in  $\text{Ba}_{0.6}\text{K}_{0.4}\text{Fe}_2\text{As}_2$  according to ARPES measurements [136]. Shown below are Fermi surfaces (ARPES intensity); temperature dependences of gaps on different sheets of the Fermi surface are plotted in the inset above.

practically isotropic on appropriate sheets of the Fermi surface. Accordingly, the  $2\Delta/T_c$  ratio is different on different sheets (cylinders) and formally is consistent with both strong (large gap, the ratio is 7.5) and weak (small gap, the ratio is 3.7) coupling. These results correspond to the picture of generalized s-wave pairing, which will be discussed below.

Quite similar results for gap widths on different sheets of the Fermi surface were also obtained in Ref. [137] through ARPES measurements on single crystals of  $(\text{Sr/Ba})_{1-x}\text{K}_x\text{Fe}_2\text{As}_2$ . Also in this work, the electron dispersion was measured by ARPES in a rather wide energy interval, which demonstrated the presence of characteristic ‘kinks’ attributed to conduction electron interaction with collective oscillations (phonons or spin excitations), allowing determination of electron velocity in the neighborhood of the Fermi level:  $v_F \sim 0.7 \pm 0.1$  eV  $\text{\AA}$ , so that using the width of the ‘large’ gap,  $\Delta \sim 12 \pm 2$  meV, gives an estimate of coherence length (the size of the Cooper pairs)  $\xi_0 = \hbar v_F / \Delta < 20$   $\text{\AA}$ , i.e., a relatively small value (compact pairs).

Rather unexpected results for the topology of Fermi surfaces were obtained in Refs [139, 140] for  $\text{Ba}_{1-x}\text{K}_x\text{Fe}_2\text{As}_2$ , where Fermi surface sheets close to the M point were discovered to have a characteristic ‘propeller’-like form which does not agree with any LDA band calculations. Measurements of the superconducting gap width in Ref. [140] for the ‘large’ gap on an ‘internal’ hole-like cylinder around point  $\Gamma$  have given the value of  $\Delta \sim 9$  meV, and the same value on propeller blades close to the M points, which corresponds to the ratio  $2\Delta/T_c = 6.8$ . On an ‘external’ hole-like cylinder around point  $\Gamma$ , the value of  $\Delta < 4$  meV was obtained, corresponding to  $2\Delta/T_c < 3$ .

Notice also Ref. [142] where ARPES measurements were performed on the ‘maximally doped’ variant of the  $\text{Ba}_{1-x}\text{K}_x\text{Fe}_2\text{As}_2$  system with  $x = 1$ , i.e., on superconducting  $\text{KFe}_2\text{As}_2$  compound ( $T_c = 3$  K). It was revealed that the form of hole-like Fermi surfaces (sheets) surrounding the  $\Gamma$  point is qualitatively the same as in  $\text{Ba}_{1-x}\text{K}_x\text{Fe}_2\text{As}_2$  with  $x = 0.4$

( $T_c = 37$  K), while electron-like cylinders surrounding the M points are simply absent. This is a natural consequence of the downward shift of the Fermi level due to hole doping (cf. Fig. 21, where it is clearly seen that electronic branches of the spectrum are above the Fermi level, where it has a big enough downward energy shift). Furthermore, similarly to Ref. [134], the observed bands turned out to be significantly (2–4 times) narrower than those obtained in all LDA type calculations. This fact, as already noted above, most probably points to sufficiently strong electronic correlations (see Section 3.4). The absence of electronic pockets on the Fermi surface leads to the disappearance of interband mechanisms of pairing (see below) and a corresponding significant lowering of  $T_c$ .

Summing up, it should be emphasized that the results of ARPES studies of Fermi surfaces and the electronic spectrum of FeAs-based superconductors are in quite satisfactory agreement with LDA calculations of band structure. Remaining inconsistencies are most probably due to the unaccounted role of electronic correlations and, sometimes, due to insufficient resolution in the ARPES experiments.

Unfortunately, thus far there have been almost no experiments on determining the Fermi surfaces from low-temperature quantum oscillations (like de Haas–van Alphen effect). We can only mark Ref. [143] where the nonsuperconducting phase of  $\text{SrFe}_2\text{As}_2$  was studied and the oscillation periods discovered corresponded to small Fermi surface pockets, which apparently can be attributed to hole-like cylinders close to the  $\Gamma$  point, almost completely ‘closed’ by the antiferromagnetic gap. In Ref. [144], quantum oscillations were studied in the  $\text{LaOFeP}$  compound and found to be in agreement with the Fermi surface predicted by LDA calculations, with due regard for an effective mass enhancement by approximately two times.

### 3.4 Correlations (LDA + DMFT)

LDA calculations of electronic spectrum neglect the potentially strong effects of local electron correlations (Hubbard–like repulsion of electrons), which can be naturally expected in bands formed mainly from d-states of Fe in FeAs layers. At present, the most consistent approach to the analysis of such correlations is considered to be the dynamical mean field theory (DMFT) [145–149], including its variant (LDA + DMFT) taking into account the LDA band structure of real systems [150–152].

The LDA + DMFT approach was employed in calculating the electronic structure of FeAs-based compounds in Refs [153–157]. In all of these, except for Ref. [156], only the  $\text{LaOFeAs}$  system was studied, while in Ref. [156] the authors analyzed the  $\text{REOFeAs}$  ( $RE = \text{La, Ce, Pr, Nd}$ ) series.

In Ref. [153], LDA + DMFT was utilized to calculate the spectral density and optical conductivity of  $\text{LaO}_{1-x}\text{F}_x\text{FeAs}$ . The magnitude of Hubbard repulsion was taken to be  $U = 4$  eV, while the Hund (exchange) coupling was assumed to be equal to  $J = 0.7$  eV<sup>5</sup>. In Fig. 28 we gave the results for the momentum dependence of the spectral density in high-symmetry directions in the Brillouin zone. The positions of the maxima of spectral density describe the effective dispersion of (damped) quasiparticles, which may be compared with the results of LDA calculations (infinite lifetime quasiparticles), which are also presented. Doping was described in the virtual crystal approximation. It can be ascertained that

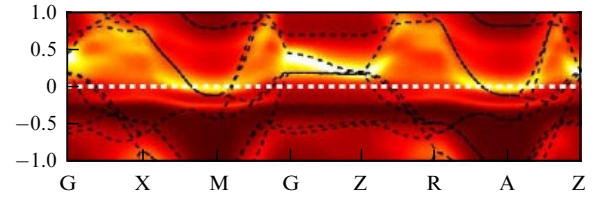


**Figure 28.** Momentum dependence of spectral density (with positions of the maxima defining the effective dispersion of quasiparticles) in the LDA + DMFT approximation for  $\text{LaOFeAs}$  with 10% doping. Dashed lines fit the results of the LDA approach [154].

electron correlations lead to a significant (3–5 times) enhancement of effective masses and strong damping of quasiparticles. The system remains metallic, though a kind of ‘bad’ metal with a strongly renormalized quasiparticle amplitude (residue at the Green’s function pole)  $Z \sim 0.2 - 0.3$ .

The general picture of the spectrum displayed in Fig. 28 can be qualitatively compared with ARPES data given in the lower part of Fig. 26b. Though the experiment was carried out on another system, a certain similarity is obvious — conduction bands are significantly narrowed (in comparison with LDA results), while in the energy region around  $-0.5$  eV the bands are simply ‘destroyed’ and a kind of energy gap reveals itself there.

According to Ref. [153], even a rather small enhancement of the Hubbard repulsion up to  $U = 4.5$  eV transforms this system into a kind of Mott insulator with an energy gap at the Fermi level. Thus, it was concluded that the systems under consideration are characterized by intermediate correlations and are close to the Mott insulator, making them partly similar to HTSC cuprates. At the same time, contrary to cuprates, prototype (undoped) compounds constitute metals, not Mott insulators.

A quite different conclusion was reached by the authors of Ref. [154], who performed formally the same type of calculations (by the same methods and with the same choice of parameters). It was claimed in this work that even the use of  $U$  values up to 5 eV does not transform a system into a Mott insulator, and changes in spectral density (electron dispersion) and the density of states due to electron correlations are rather insignificant.

At present, the reasons for such drastic differences in the results obtained by two leading groups making LDA + DMFT calculations are unclear.

In general, it should be noted that the *ab initio* nature of LDA + DMFT approach is rather conditional, as, for example, the magnitude of Hubbard interaction  $U$  is, in fact, a kind of (semi)phenomenological parameter. There exist a number of *ab initio* approaches to calculating its magnitude, of which the most consistent is assumed to be the so-called method of constrained random phase approximation (constrained RPA) [158, 159]. Within this approach the magnitude of local Hubbard repulsion is calculated from the ‘bare’ Coulomb repulsion  $V$  using the RPA expression

$$U = \frac{V}{1 - V\Pi_r}, \quad (6)$$

where  $\Pi_r$  is the polarization operator taking into account screening by electrons from the outside of the (correlated)

<sup>5</sup> The DMFT impurity problem was solved by the quantum Monte Carlo (QMC) method with the temperature taken to be 116 K.

**Table 4.** ‘Bare’ and partly screened Coulomb interactions  $V$  and  $U$ , and Hund coupling  $J$  for LaOFeAs, obtained in Ref. [156] by excluding different groups of states (listed in the first column) from screening.

	$V$ , eV	$U$ , eV	$J$ , eV
d	15.99	2.92	0.43
dpp	20.31	4.83	0.61
d-dpp	20.31	3.69	0.58

bands of interest. For example, if we limit ourselves only to the analysis of bands formed by d-states of Fe, we have to use the relation  $\Pi_r = \Pi - \Pi_d$ , where  $\Pi_d$  is the polarization operator calculated only on d-states. It is clear that the magnitude of  $U$  defined in this way depends essentially on the adopted scheme of calculations (accounting for the contribution from different groups of electrons to screening).

For FeAs-based compounds, this problem was studied in Ref. [156]. The values of different interaction parameters entering the LDA + DMFT calculation scheme, obtained by the exclusion of different groups of states from the screening of the bare Coulomb interaction, are given in Table 4.

It is readily seen that the magnitudes of interaction parameters entering LDA + DMFT calculation scheme can change within rather wide ranges.

The same questions were discussed in Refs [155, 157] (within the constrained DFT approach [160]), with the authors coming to the conclusion that the effective parameters of Coulomb (Hubbard) repulsion are relatively small if we limit ourselves to the framework of d-states of Fe. Accordingly, the LDA + DMFT calculations performed in these works produced an electronic structure which is only slightly different from LDA results.

In the opinion of the authors of Refs [154, 155, 157], their conclusion about the smallness of electron correlations in FeAs-based systems is confirmed by experiments on X-ray absorption and emission spectroscopy in Ref. [161]; however, this is in sharp contrast to available ARPES data [134, 141] which definitely indicate rather strong renormalization of the electronic spectrum due to correlations. It should be stressed that data on the topology of Fermi surfaces are, in fact, insufficient for making any judgments on the role of correlations: Fermi surfaces in the LDA + DMFT approach are just the same as in the LDA approximation. It is important to study in detail electronic dispersion, bandwidths, and quasiparticle damping far enough from the Fermi level, as well as quasiparticle residue  $Z$ . In our opinion, ARPES measurements have many advantages here and can help in solving this important problem.

Summarizing, the question of the role of electron correlations in new superconductors is still under discussion. It is most probable that correlations in these systems are of intermediate strength between typical metals and systems like Mott insulators, so that we are dealing here with the state of a *correlated* metal [147, 149].

### 3.5 Spin ordering: localized or itinerant spins?

In this section we shall briefly consider theoretical ideas on the nature of antiferromagnetic ordering in undoped FeAs-based compounds and the closely related problem of the structural transition from the tetragonal to orthorhombic phase. Broadly speaking, these questions are slightly outside the scope of our review (superconductivity in FeAs-based compounds), so our presentation will be very short.

The possibility of antiferromagnetic ordering in the systems under consideration had been noted even before the direct neutronographic observations discussed in Section 2.3 were made. Already in one of the earliest papers on the electronic structure of iron oxypnictides [110], as well as during the analysis of the ‘minimal’ two-band model [127], it was stressed that there is an approximate ‘nesting’ of hole-like Fermi surfaces around point  $\Gamma$  and electron-like Fermi surfaces around M points. It is most easily seen, for instance, in Fig. 23c — the shift of the hole-like cylinder by vector  $(\pi, 0)$  or  $(0, \pi)$  leads to its approximate coincidence with the electron-like cylinder. Direct calculations [110, 127] revealed that this fact leads to the formation of a rather wide, but still quite noticeable, peak in static magnetic susceptibility  $\chi_0(\mathbf{q})$  (determined by the appropriate loop diagram) at  $\mathbf{q} = (\pi, 0)$  and  $\mathbf{q} = (0, \pi)$ . In turn, this may lead to antiferromagnetic instability accompanied by the formation of a spin density wave (SDW) with the appropriate wave vector, at least in the case of a sufficiently strong exchange interaction. We have seen above that precisely this type of spin ordering was established experimentally in FeAs layers [69, 71, 74, 76–78]. Also, the observed, rather small values of magnetic moments on Fe provide evidence of the itinerant nature of magnetism (SDW). It is also natural to assume that well-developed spin fluctuations of the SDW type persist in doped (superconducting) compounds, which can provide the pairing interaction of electrons.

At the same time, magnetic ordering in FeAs layers can also be analyzed within a more traditional approach based on the qualitative picture of localized spins on Fe ions, interacting via the usual Heisenberg exchange between nearest and second nearest neighbors. Such an analysis was performed, for instance, in Ref. [162] for LaOFeAs, as well as *ab initio* calculations of appropriate exchange integrals and values of magnetic moments. For us here, the qualitative aspects of this analysis, which are illustrated in Fig. 29, are more important [162].

In this figure we displayed two possible antiferromagnetic configurations of spins in the FeAs layer. In the experiments [69], the AF2 (see Fig. 29) type spin structure is observed, which is realized when inequality  $J_1 < 2J_2$  holds, where  $J_1$  is an exchange integral between nearest neighbors, and  $J_2$  between second nearest neighbors, with both integrals assumed positive (antiferromagnetism). Direct (FP-LAPW) calculations of the total ground state energy of LaOFeAs, performed in Ref. [162], confirmed the greater stability of precisely this state. AF2 configuration can be considered as two interpenetrating antiferromagnetic square sublattices shown by different colors in Fig. 29. In this case, each Fe ion

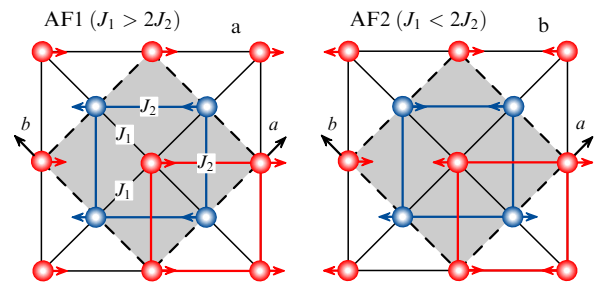


**Figure 29.** Two alternative spin configurations in the antiferromagnetic FeAs layer: (a) antiparallel spins on nearest neighbors, and (b) antiparallel spins on second nearest neighbors [162].

is placed at the center of an antiferromagnetically ordered cell, so that the mean molecular field acting on its spin is just zero. Therefore, each sublattice may freely (with no expenditure of energy) rotate with respect to the other. This is a situation of complete frustration. It is well known that such a state is usually unstable with respect to structural distortions. Thus, it can be expected that a structural distortion will appear in our system, making the spins of a pair of Fe ions closer to each other, while the pair on the other side of the square slightly farther apart. This is just the type of distortion (tetra–ortho transition) observed in the experiment [69]. Direct calculations of total energy confirm this assumption [162].

However, the general situation with the nature of magnetic ordering and structural transition in FeAs layers is rather far from being completely clear. *Ab initio* calculations as a rule produce highly overestimated values of magnetic moments on Fe, while the relative stability of magnetic structures strongly depends on the details of the methods used. Apparently, this is due to the itinerant nature of magnetism in these systems. Detailed discussions of these problems can be found in interesting papers [163, 164] where an original qualitative picture of strong magnetic fluctuations was proposed, allowing, in the authors' opinion, the explanation of all the anomalies of magnetic properties.

#### 4. Mechanisms and types of pairing

After the discovery of high-temperature superconductivity in iron-based layered compounds, dozens of theoretical papers appeared with different proposals for the possible microscopic mechanisms and types of Cooper pairing in these systems. A review of all these papers here is impossible and below we shall deal only with a very few of, in our opinion, the most important works.

##### 4.1 Multiband superconductivity

The main distinction of new superconductors is their multiple band nature. An electronic structure in a narrow enough energy interval around the Fermi level is formed practically only from the d-states of Fe. The Fermi surface consists of several hole-like and electron-like cylinders and on each its 'own' energy gap can be formed. Broadly speaking, this situation is not new and has already been analyzed in the scientific literature [165]. For the specific band structure typical of FeAs layers, however, we need an additional analysis.

In general, a sufficient formulation of this problem was considered in a paper by Barzykin and Gor'kov [166], and some of their results will be presented below. A typical electronic spectrum of FeAs-layered systems in the relevant (for superconductivity) energy interval was displayed in Fig. 21. A similar, in principle, spectrum was also obtained in the minimal model of Ref. [127]. An oversimplified view of this spectrum is represented in Fig. 30 [166].

This form of Fermi surfaces corresponds to the stoichiometric (undoped) composition of these compounds, with electrons and holes occupying the same volumes (compensated semimetal).<sup>6</sup> Electronic doping shrinks hole-like pockets, while hole doping shrinks electron-like pockets.

<sup>6</sup> In fact, this very form of the spectrum was assumed in numerous papers on excitonic instability and the excitonic insulator [167–171]. This instability may be considered as an alternative explanation of antiferromagnetic ordering and structural transition in these systems [166].

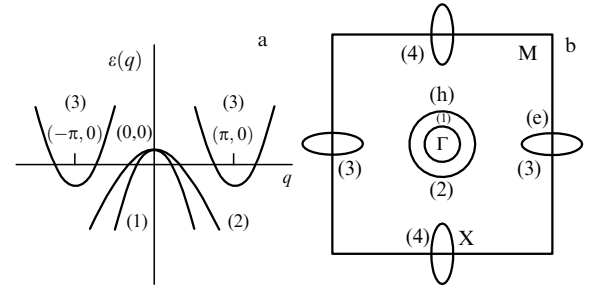


**Figure 30.** Schematic views of electronic spectrum (a) and Fermi surfaces (b) for LaOFeAs in the extended band picture. Around point  $\Gamma$  there are two hole-like sheets, while electron-like sheets are around  $X$  points [166].

In Ref. [166], a symmetry analysis of possible types of superconducting order parameter was performed along the lines of Refs [172, 173], and also the explicit solutions of BCS equations were found for a system with the electronic spectrum shown in Fig. 30.

Let  $\Delta_i(\mathbf{p})$  be a superconducting order parameter (gap) on the  $i$ th sheet of the Fermi surface. The value of  $\Delta_i(\mathbf{p})$  is determined by the self-consistency equation for the anomalous Gor'kov's function  $F_i(\omega_n, \mathbf{p})$ :

$$\Delta_i(\mathbf{p}) = T \sum_{j, \omega_n} \int d\mathbf{p}' V^{i,j}(\mathbf{p} - \mathbf{p}') F_j(\omega_n, \mathbf{p}'), \quad (7)$$

where  $V^{i,j}(\mathbf{p} - \mathbf{p}')$  is the pairing interaction. If Fermi surface pockets are sufficiently small (as they seem to be in FeAs-based systems), transferred momentum  $\mathbf{p} - \mathbf{p}'$  is also small within each pocket and we can replace  $V^{i,j}(\mathbf{p} - \mathbf{p}')$  by  $V^{i,j}(0)$ , which is favorable for the formation of momentum-independent gaps.

Pairing BCS interaction in this model can be represented by the following matrix

$$V = \begin{pmatrix} u & u & t & t \\ u & u & t & t \\ t & t & \lambda & \mu \\ t & t & \mu & \lambda \end{pmatrix}, \quad (8)$$

where  $\lambda = V^{eX, eX} = V^{eY, eY}$  defines interaction in an electron-like pocket at point  $X$ ,  $\mu = V^{eX, eY}$  connects electrons from different pockets at points  $(\pi, 0)$  and  $(0, \pi)$ ,  $u = V^{h1, h1} = V^{h2, h2} = V^{h1, h2}$  characterizes BCS interaction in two hole-like pockets<sup>7</sup> surrounding the point  $\Gamma$ , and  $t = V^{h, eX} = V^{h, eY}$  connects electrons from points  $X$  and  $\Gamma$ .

The critical temperature  $T_c$  of superconducting transition is determined by the solution of the system of linearized gap equations:

$$\Delta_i = \sum_j \bar{V}^{i,j} \Delta_j \ln \frac{2\gamma\bar{\omega}}{\pi T_c}, \quad (9)$$

where  $\bar{\omega}$  is the usual cut-off frequency of logarithmic divergence in the Cooper channel, and

$$\bar{V}^{i,j} \equiv -\frac{1}{2} V^{i,j} v_j, \quad (10)$$

where  $v_j$  is the density of states on the  $j$ th sheet (pocket) of the Fermi surface.

<sup>7</sup> An assumption that these couplings are the same seems to us to be too rigid.

Introducing an effective coupling constant  $g$  and writing down  $T_c$  as

$$T_c = \frac{2\gamma\bar{\omega}}{\pi} \exp\left(-\frac{2}{g}\right), \quad (11)$$

we arrive at the solutions of three types:

(1) solution corresponding to  $d_{x^2-y^2}$  symmetry, when gaps on different pockets at points X differ in signs, while gaps on hole-like pockets are zero:

$$\Delta_1 = \Delta_2 = 0, \quad \Delta_3 = -\Delta_4 = \Delta, \quad (12)$$

$$g = (\mu - \lambda) v_3. \quad (13)$$

The possibility of such a solution follows also from the general symmetry analysis [166];

(2) two solutions corresponding to the so-called  $s^\pm$ -pairing, when gaps at points X have the same sign, while gaps on the Fermi surfaces surrounding point  $\Gamma$  may have opposite signs, namely<sup>8</sup>

$$2g_{+,-} = -u(v_1 + v_2) - (\lambda + \mu) v_3 \pm \sqrt{(u(v_1 + v_2) - (\lambda + \mu) v_3)^2 + 8t^2 v_3(v_1 + v_2)} \quad (14)$$

and

$$\Delta_1 = \Delta_2 = \kappa\Delta, \quad \Delta_3 = \Delta_4 = \Delta, \quad (15)$$

where  $\kappa^{-1} = -(g_{+,-} + u(v_1 + v_2))/(tv_3)$ .

The possibility of  $s^\pm$ -pairing in FeAs-based compounds was first noted in Ref. [110]. This solution is in qualitative agreement with available ARPES data [136, 137, 140], except for the results  $\Delta_1 = \Delta_2$  from Eqn (15), which contradict the established fact that the gap on a small hole-like cylinder is approximately twice as large as on a big cylinder. In our opinion, this drawback is due to the unnecessary limitation of  $u = \mathcal{V}^{h1,h1} = \mathcal{V}^{h2,h2} = \mathcal{V}^{h1,h2}$ , used in Ref. [166]. For different BCS constants on hole-like cylinders we can easily obtain different values of the gap width, in agreement with experiments.

The presence of practically isotropic gaps (possibly of different signs) on hole-like and electron-like pockets of the Fermi surface, corresponding to  $s^\pm$ -pairing, seems at first to contradict the numerous NMR (NQR) data discussed in Section 2.5, which indicate possible d-wave gap symmetry. This contradiction was studied in Ref. [174], where it was shown rather convincingly that the absence of a Gabel–Slichter peak and power-like temperature dependence of NMR relaxation may also be easily explained in the case of  $s^\pm$ -pairing, taking into account impurity scattering.

## 4.2 Electron–phonon mechanism

The general discussion in the previous section tells us nothing about the origin of pairing coupling constants entering into the matrix (8), i.e., about the microscopic mechanism of Cooper pairing in new superconductors.

As a first candidate for such a mechanism we have to consider the conventional electron–phonon interaction. Such an analysis for LaOFeAs was performed in Ref. [109] using *ab initio* calculations of electron and phonon spectra

and the Eliashberg function  $\alpha^2F(\omega)$  determining the electron–phonon pairing constant as

$$\lambda(\omega) = 2 \int_0^\omega d\Omega \frac{\alpha^2F(\Omega)}{\Omega}. \quad (16)$$

The total electron–phonon pairing constant  $\lambda$  was obtained by numerical integration in formula (16) up to  $\omega = \infty$  and was found to be 0.21. To estimate superconducting critical temperature  $T_c$  we can use a popular Allen–Dynes interpolation formula [175]:

$$T_c = \frac{f_1 f_2 \omega_{\text{ln}}}{1.20} \exp\left(-\frac{1.04(1+\lambda)}{\lambda - \mu^* - 0.62\lambda\mu^*}\right), \quad (17)$$

where

$$f_1 = \left[1 + \left(\frac{\lambda}{A_1}\right)^{3/2}\right]^{1/3}, \quad A_1 = 2.46(1 + 3.8\mu^*),$$

$$f_2 = 1 + \frac{(\bar{\omega}_2/\omega_{\text{ln}} - 1)\lambda^2}{\lambda^2 + A_2^2}, \quad A_2 = 1.82(1 + 6.3\mu^*) \frac{\bar{\omega}_2}{\omega_{\text{ln}}},$$

$$\bar{\omega}_2 = \langle\omega^2\rangle^{1/2},$$

and  $\langle\omega^2\rangle$  is the average square of the phonon frequency. Taking into account the value of the average logarithmic frequency of phonons,  $\omega_{\text{ln}} = 205$  K (and assuming  $\omega_{\text{ln}} \approx \bar{\omega}_2$ ), found in Ref. [109], and with the optimistic choice of Coulomb pseudopotential  $\mu^* = 0$ , formula (17) gives the value of  $T_c = 0.5$  K. Numerical solution of Eliashberg equations with the calculated function  $\alpha^2F(\omega)$  gave the value of  $T_c = 0.8$  K [109]. Actually, to reproduce the experimental value of  $T_c = 26$  K, coupling constant  $\lambda$  should be approximately five times larger, even if we set  $\mu^* = 0$ . In the opinion of the authors of Ref. [109], such a strong discrepancy clearly indicates that the usual picture of Cooper pairing, based on electron–phonon coupling, is invalid.

Despite the quite convincing estimates of Ref. [109], it should be noted that these are based on the standard approach of the Eliashberg theory, which does not take into account, in particular, the important role of the multiband nature of superconductivity in these compounds, and possibly the importance of interband pairing interactions. Moreover, the estimates of the value of the electron–phonon coupling constant has also met with objections. Thus, it was argued in Ref. [176] that sufficiently strong coupling exists between electrons and a certain mode of Fe oscillations in the FeAs plane.

However, probably the most convincing objections to the claims of irrelevance of electron–phonon coupling can be based on experiments. In particular, we can estimate the electron–phonon coupling constant from the temperature dependence of resistivity. The measurements of resistivity of PrFeAsO<sub>1-x</sub>F<sub>x</sub> were done in Ref. [177] in a satisfactorily wide temperature interval. Linear growth in resistivity with temperature for  $T > 170$  K was saturated, which by itself suggests strong enough electron–phonon coupling. As a simple estimate, we can write down resistivity as

$$\rho(T) = \frac{4\pi}{\omega_p^2 \tau}, \quad (18)$$

where  $\omega_p$  is the plasma frequency, and  $\tau$  is the carrier relaxation time. In the region of sufficiently high tempera-

<sup>8</sup> Here, we have corrected small misprints in Ref. [166].

tures, where resistivity grows linearly with temperature, the relaxation frequency of carriers on phonons is given by [178]

$$\frac{\hbar}{\tau_{\text{ep}}} = 2\pi\lambda_{\text{tr}}k_{\text{B}}T, \quad (19)$$

where ‘transport’ constant  $\lambda_{\text{tr}}$  of electron–phonon coupling is naturally on the order of  $\lambda$  of interest to us, usually differing from it by no more than 10%. From formulas (18) and (19) we have

$$\lambda_{\text{tr}} = \frac{\hbar\omega_{\text{p}}^2}{8\pi^2k_{\text{B}}} \frac{d\rho}{dT}. \quad (20)$$

Using the slope of the temperature dependence of resistivity determined in Ref. [177],  $d\rho/dT \sim 8.6 \mu\Omega \text{ K}^{-1}$ , and the estimate of plasma frequency  $\omega_{\text{p}} \sim 0.8 \text{ eV}$  (which follows from measurements of penetration depth), we get  $\lambda \sim 1.3$ , which, according to formula (17), is quite sufficient for getting the observable values of transition temperatures in new superconductors.

Decisive evidence for the electron–phonon mechanism of Cooper pairing was always considered to be the observation of the isotope effect. Appropriate measurements were performed recently in Ref. [179] on  $\text{SmFeAsO}_{1-x}\text{F}_x$ , where  $^{16}\text{O}$  was replaced by  $^{18}\text{O}$ , and on  $\text{Ba}_{1-x}\text{K}_x\text{Fe}_2\text{As}_2$ , where  $^{54}\text{Fe}$  was substituted for  $^{56}\text{Fe}$ . A finite shift in superconducting transition temperature was observed, which can be characterized in a standard way by the isotope effect exponent  $\alpha = -d \ln T_{\text{c}}/d \ln M$ . For  $\text{SmFeAsO}_{1-x}\text{F}_x$ , the isotope effect turned out to be small enough, with  $\alpha \sim 0.08$ , which is quite natural as O ions reside exterior to the conducting FeAs layer. At the same time, the replacement of Fe ions in FeAs layers in  $\text{Ba}_{1-x}\text{K}_x\text{Fe}_2\text{As}_2$  has led to a large isotope effect with  $\alpha \approx 0.4$ , which is close to the ‘ideal’ value of  $\alpha = 0.5$ .

Thus, the rather wide pessimism in the literature on the role of electron–phonon interactions in new superconductors seems to be rather premature.

### 4.3 Magnetic fluctuations

The above-mentioned pessimism with respect to the role of electron–phonon interactions, as well as the closeness of the superconducting phase to the antiferromagnetic phase in the phase diagram of new superconductors, has led to the growth of popularity of pairing models based on the decisive role of magnetic (spin) fluctuations, being in many respects similar to those already considered for HTSC cuprates [4, 5].

Apparently, one of the first papers where the possible role of magnetic fluctuations in the formation of Cooper pairs of the  $s^{\pm}$  type was stressed at the qualitative level was Ref. [110]. Similar conclusions were reached by the authors of Ref. [123], where the possibility of  $d_{x^2-y^2}$ -pairing was also noticed.

A rather detailed analysis of possible electronic mechanisms of pairing within the generalized Hubbard Hamiltonian applied to the minimal model of Ref. [127] was performed in Ref. [180]. In fact, this analysis was done in the framework of the generalized RPA approximation which takes into account an exchange by spin (and orbital) fluctuations in the particle–hole channel (cf. the review of similar one-band models utilized for cuprates [4]). It was shown that the pairing interaction due to these fluctuations leads to effective attraction in the case of singlet d-wave pairing and triplet p-wave pairing, with the tendency to d-wave pairing instability becoming stronger as the system moves towards magnetic

(SDW) instability. In a rather general formulation, using the general renormalization group approach, a similar model was analyzed in Ref. [181].

Unfortunately, in most of the papers devoted to the pairing mechanism due to the exchange of magnetic fluctuations there are no direct calculations of  $T_{\text{c}}$  allowing comparison with experiments. Thus, we shall limit ourselves to these short comments.

## 5. Conclusion: end of cuprate monopoly

Let us briefly summarize. During the first six months of studies of new superconductors we have observed rather impressive progress in learning about their basic physical properties. Very few problems remain noninvestigated, though many results obtained require further clarification.<sup>9</sup> The main result of all these studies is certainly the end of the cuprate monopoly in the physics of high-temperature superconductivity. A new wide class of iron-based systems was discovered with high enough values of  $T_{\text{c}}$  and a variety of physical properties, which brings to mind copper oxides that for more than 20 years were the center of interest of the superconductor community. There are rather well-founded expectations that in some near future new systems will also be discovered, though there is now a certain impression that in the subclass of layered FeAs systems we have already reached the maximum values of  $T_{\text{c}} \sim 50 \text{ K}$ , so that for further enhancement of  $T_{\text{c}}$  we need some kind of a new approaches. Doubtless, the work already done has significantly deepened our understanding of the nature of high-temperature superconductivity, though we are still far from formulation of definite ‘recipes’ in the search for new superconductors with higher values of  $T_{\text{c}}$ .

Let us formulate

### What do iron-based and cuprate superconductors have in common?

- Both classes are represented by quasi-two-dimensional (layered) systems from the point of view of their electronic properties, which leads to more or less strong anisotropy.
- In both classes, the superconducting region in the phase diagram is close to the region of antiferromagnetic ordering. The prototype phase for both classes of superconductors is antiferromagnetic.
- Cooper pairing in both classes is of the singlet type, but ‘anomalous’, i.e., different from the simple s-wave pairing characteristic of traditional (low-temperature) superconductors.
- The basic properties of the superconducting state is more or less the same as in typical type II superconductors.

From the point of view of our understanding of the basic nature of high-temperature superconductivity, the meaning of these common properties remains rather unclear. Why do we need (and do we need?) two-dimensionality? Historically, the importance of two-dimensionality was first stressed in connection with the proposed high-temperature superconductivity based on the excitonic mechanism of Ginzburg and Little [182], but does it play any significant role for superconductivity in HTSC cuprates and new iron-based superconductors? Do we need ‘closeness’ to antiferromagnetism? Is antiferromagnetism just a competing phase, or is it helpful for

<sup>9</sup> In this respect, we want to stress the absence of any systematic studies on the disordering effects which may be unusual due to the anomalous nature of  $s^{\pm}$ -pairing.

HTSC, for example, via the replacement of electron – phonon pairing by a mechanism based on spin (antiferromagnetic) fluctuations? The answers to these questions are still unclear, though the presence of such coincidences in rather different classes of physical systems seem rather significant.

Let us now look

#### What is the difference between iron-based and cuprate superconductors?

- Prototype phases of HTSC cuprates are antiferromagnetic (strongly correlated, Mott type) insulators, while for new superconductors these are antiferromagnetic (intermediately correlated?) metals.

- Cuprates in the superconducting state are one-band metals with a single Fermi surface (hole-like or electron-like), while new superconductors are multiple band metals with several hole-like and electron-like Fermi surfaces.

- In cuprates, we have anisotropic d-wave pairing, while in new superconductors, almost surely, we have (almost?) isotropic  $s^{\pm}$ -pairing.

- It is quite possible that the microscopic mechanism of pairing in both classes of superconductors is different: in cuprates it is almost certainly an electronic mechanism (spin fluctuations), while in iron-based superconductors the role of electron – phonon coupling can be quite important (the isotope effect!).

It is evident that the differences between cuprates and new superconductors are probably more pronounced than are their common properties. In this sense, one of the main conclusions which can already be made is that HTSC is not a unique property of cuprates, i.e., strongly correlated systems close to the insulating state. In some respects, new superconductors are simpler and easier to understand — their normal state is not so mysterious as in the case of cuprates,<sup>10</sup> though their multiple band structure complicates situation.

To conclude, it is believed that high-temperature superconductivity is much more common than has been assumed during the last 20 years, so that the high-temperature superconductor community may look into the future with certain optimism.

The author is grateful to L P Gor'kov and I I Mazin for numerous discussions on the physics of new superconductors. He is also grateful to I A Nekrasov and Z V Pchelkina, who co-authored papers on calculations of electronic spectra of FeAs-based systems. This work was partly supported by the Russian Foundation for Basic Research, grant No. 08-02-00021, and by the programs of fundamental research of the Russian Academy of Sciences, titled 'Quantum Macrophysics' and 'Strongly Correlated Electrons in Semiconductors, Metals, Superconductors, and Magnetic Materials'.

## References

1. Bednorz J G, Müller K A Z. *Phys. B* **64** 189 (1986)
2. Gor'kov L P, Kopnin N B *Usp. Fiz. Nauk* **156** 117 (1988) [*Sov. Phys. Usp.* **31** 850 (1988)]
3. Izyumov Yu A, Plakida N M, Skryabin Yu N *Usp. Fiz. Nauk* **159** 621 (1989) [*Sov. Phys. Usp.* **32** 1060 (1989)]
4. Izyumov Yu A *Usp. Fiz. Nauk* **161** (11) 63 (1991) [*Sov. Phys. Usp.* **34** 935 (1991)]

<sup>10</sup> Some evidence for the pseudogap state was observed only in NMR data and it is unclear whether in new superconductors we have an additional pseudogap region in the phase diagram as in cuprates, with appropriate renormalization of the electronic spectrum, like, formation of 'Fermi arcs', etc.

5. Izyumov Yu A *Usp. Fiz. Nauk* **169** 225 (1999) [*Phys. Usp.* **42** 215 (1999)]
6. Maksimov E G *Usp. Fiz. Nauk* **170** 1033 (2000) [*Phys. Usp.* **43** 965 (2000)]
7. Sadovskii M V *Usp. Fiz. Nauk* **171** 539 (2001) [*Phys. Usp.* **44** 515 (2001)]
8. Belyavskii V I, Kopaev Yu V *Usp. Fiz. Nauk* **176** 457 (2006) [*Phys. Usp.* **49** 441 (2006)]
9. Maksimov E G *Usp. Fiz. Nauk* **178** 175 (2008) [*Phys. Usp.* **51** 167 (2008)]
10. Kopaev Yu V, Belyavskii V I, Kapaev V V *Usp. Fiz. Nauk* **178** 202 (2008) [*Phys. Usp.* **51** 191 (2008)]
11. Plakida N M *Vysokotemperaturnye Sverkhprovodniki* (High-Temperature Superconductivity) (Moscow: Mezhdunarodnaya Programma Obrazovaniya, 1996) [Translated into English (Berlin: Springer-Verlag, 1995)]
12. Anderson P W *The Theory of Superconductivity in the High-T<sub>c</sub> Cuprates* (Princeton, NJ: Princeton Univ. Press, 1997)
13. Schrieffer J R (Ed.) *Handbook of High-Temperature Superconductivity* (New York: Springer, 2007)
14. Bennemann K, Ketterson J B (Eds) *Superconductivity Vols 1, 2* (Berlin: Springer-Verlag, 2008)
15. Kamihara Y et al. *J. Am. Chem. Soc.* **130** 3296 (2008)
16. Shaked H et al. *Crystal Structures of the High-T<sub>c</sub> Superconducting Copper-Oxides* (Amsterdam: Elsevier Science B.V., 1994)
17. Sadovskii M V "Modeli psevdoshchelevogo sostoyaniya v vysokotemperaturnykh sverkhprovodnikov" ("Models of the pseudogap state in high-temperature superconductors"), in *Struny, Brany, Reshetki, Setki, Psevdoshcheli i Pylinki: Trudy Seminara im. I.E. Tamma* (Strings, Branes, Lattices, Nets, Pseudogaps and Dust. Proc. I E Tamm Seminar) (Moscow: Nauchnyi Mir, 2007) pp. 357 – 441; Sadovskii M V, cond-mat/0408489
18. Hüfner S et al. *Rep. Prog. Phys.* **71** 062501 (2008)
19. Pennington C H, Stenger V A *Rev. Mod. Phys.* **68** 855 (1996)
20. Mackenzie A P, Maeno Y *Rev. Mod. Phys.* **75** 657 (2003)
21. Ovchinnikov S G *Usp. Fiz. Nauk* **173** 27 (2003) [*Phys. Usp.* **46** 21 (2003)]
22. Vinod K, Varghese N, Syamaprasad U *Supercond. Sci. Technol.* **20** R31 (2007)
23. Putti M, Vaglio R, Rowell J M *Supercond. Sci. Technol.* **21** 043001 (2008)
24. Kamihara Y et al. *J. Am. Chem. Soc.* **128** 10012 (2006)
25. Watanabe T et al. *Inorg. Chem.* **46** 7719 (2006)
26. Chen G F et al. *Phys. Rev. Lett.* **101** 057007 (2008); arXiv:0803.0128
27. Zhu X et al. *Supercond. Sci. Technol.* **21** 105001 (2008)
28. Sefat A S et al. *Phys. Rev. B* **77** 174503 (2008); arXiv:0803.2528
29. Chen X H et al. *Nature* **453** 761 (2008); arXiv:0803.3603
30. Chen G F et al. *Phys. Rev. Lett.* **100** 247002 (2008); arXiv:0803.3790
31. Ren Z-A et al. *Europhys. Lett.* **82** 57002 (2008); arXiv:0803.4234
32. Chen G F et al. *Chinese Phys. Lett.* **25** 2235 (2008); arXiv:0803.4384
33. Ren Z-A et al. *Europhys. Lett.* **83** 17002 (2008); arXiv:0804.2582
34. Lu W et al. *Solid State Commun.* **148** 168 (2008); arXiv:0804.3725
35. Yang J et al. *Supercond. Sci. Technol.* **21** 082001 (2008); arXiv:0804.3727
36. Wen H-H et al. *Europhys. Lett.* **82** 17009 (2008); arXiv:0803.3021
37. Wang C et al. *Europhys. Lett.* **83** 67006 (2008); arXiv:0804.4290
38. Takahashi H et al. *Nature* **453** 376 (2008)
39. Zocco D A et al. *Physica C* **468** 2229 (2008); arXiv:0805.4372
40. Garbarino G et al., arXiv:0808.1132
41. Tegel M et al., arXiv:0810.2120
42. Han F et al., arXiv:0810.2475
43. Matsuishi S et al. *J. Phys. Soc. Jpn.* **77** 113709 (2008); arXiv:0810.2351
44. Zhu X et al., arXiv:0810.2531
45. Rotter M, Tegel M, Johrendt D *Phys. Rev. Lett.* **101** 107006 (2008); arXiv:0805.4630
46. Chen G F et al. *Chinese Phys. Lett.* **25** 3403 (2008); arXiv:0806.1209
47. Sasmal K et al. *Phys. Rev. Lett.* **101** 107007 (2008); arXiv:0806.1301
48. Alireza P L et al. *J. Phys. Condens. Matter* **21** 012208 (2009); arXiv:0807.1896
49. Sefat A S et al. *Phys. Rev. Lett.* **101** 117004 (2008); arXiv:0807.2237
50. Wang X C et al., arXiv:0806.4688
51. Tapp J H et al. *Phys. Rev. B* **78** 060505(R) (2008); arXiv:0807.2274
52. Hsu F-C et al., arXiv:0807.2369

53. Mizuguchi Y et al. *Appl. Phys. Lett.* **93** 152505 (2008); arXiv:0807.4315
54. Fang M H et al., arXiv:0807.4775
55. Kozhevnikov V L et al. *Pis'ma Zh. Eksp. Teor. Fiz.* **87** 747 (2008) [*JETP Lett.* **87** 649 (2008)]; arXiv:0804.4546
56. Ge J, Cao S, Zhang J, arXiv:0807.5045
57. Li Z et al. *Phys. Rev. B* **78** 060504(R) (2008); arXiv:0803.2572
58. Ronning F et al. *J. Phys. Condens. Matter* **20** 342203 (2008); arXiv:0807.3788
59. Klimczuk T et al., arXiv:0808.1557
60. Ozawa T C, Kauzlarich S M *Sci. Technol. Adv. Mater.* **9** 033003 (2008); arXiv:0808.1158
61. Rotter M et al. *Phys. Rev. B* **78** 020503(R) (2008); arXiv:0805.4021
62. Nomura T et al. *Supercond. Sci. Technol.* **21** 125028 (2008); arXiv:0804.3569
63. Zhigadlo N D et al. *J. Phys. Condens. Matter* **20** 342202 (2008); arXiv:0806.0337
64. Jia Y et al. *Appl. Phys. Lett.* **93** 032503 (2008); arXiv:0806.0532
65. Ni N et al. *Phys. Rev. B* **78** 014507 (2008); arXiv:0806.1874
66. Zhang S B et al., arXiv:0809.1905
67. Wang X F et al., arXiv:0806.2452
68. Yuan H Q et al., arXiv:0807.3137
69. de la Cruz C et al. *Nature* **453** 899 (2008); arXiv:0804.0795
70. Luetkens H et al., arXiv:0806.3533
71. Zhao J et al. *Nature Mater.* **7** 953 (2008); arXiv:0806.2528
72. Markert J T, Dalichaouch Y, Maple M B, in *Physical Properties of High Temperature Superconductors I* (Ed. D M Ginsberg) (Singapore: World Scientific, 1989) [Translated into Russian Vol. 1 (Moscow: Mir, 1990) p. 265]
73. Qiu Y et al., arXiv:0806.2195
74. Chen Y et al. *Phys. Rev. B* **78** 064515 (2008); arXiv:0807.0662
75. Drew A J et al., arXiv:0807.4876
76. Huang Q et al., arXiv:0806.2776
77. Zhao J et al. *Phys. Rev. B* **78** 140504(R) (2008); arXiv:0807.1077
78. Chen H et al., arXiv:0807.3950
79. Bao W et al., arXiv:0809.2058
80. Ding L et al. *Phys. Rev. B* **77** 180510(R) (2008); arXiv:0804.3642
81. Dong J K et al., arXiv:0806.3573
82. Mu G et al., arXiv:0808.2941
83. Nakai Y et al. *J. Phys. Soc. Jpn.* **77** 073701 (2008); arXiv:0804.4765
84. Fukuzawa H et al. *J. Phys. Soc. Jpn.* **77** 093706 (2008); arXiv:0806.4514
85. Mukuda H et al. *J. Phys. Soc. Jpn.* **77** 093704 (2008); arXiv:0806.3238
86. Matano K et al. *Europhys. Lett.* **83** 57001 (2008); arXiv:0806.0249
87. Ning F L et al. *J. Phys. Soc. Jpn.* **77** 103705 (2008); arXiv:0808.1420
88. Kotegawa H et al. *J. Phys. Soc. Jpn.* **77** 113703 (2008); arXiv:0808.0040
89. Chen T Y et al. *Nature* **453** 1224 (2008); arXiv:0805.4616
90. Millo O et al. *Phys. Rev. B* **78** 092505 (2008); arXiv:0807.0359
91. Pan M H et al., arXiv:0808.0895
92. Wang Y et al., arXiv:0806.1986
93. Dubroka A et al. *Phys. Rev. Lett.* **101** 097011 (2008); arXiv:0805.2415
94. Boris A V et al., arXiv:0806.1732
95. Yang J et al., arXiv:0807.1040
96. Li G et al. *Phys. Rev. Lett.* **101** 107004 (2008); arXiv:0807.1094
97. Ferrell R A, Glover R E (III) *Phys. Rev.* **109** 1398 (1958)
98. Tinkham M, Ferrell R A *Phys. Rev. Lett.* **2** 331 (1959)
99. Qiu Y et al. *Phys. Rev. B* **78** 052508 (2008); arXiv:0805.1062
100. Christianson A D et al. *Phys. Rev. Lett.* **101** 157001 (2008); arXiv:0807.3370
101. Singh D J, Du M-H *Phys. Rev. Lett.* **100** 237003 (2008); arXiv:0803.0429
102. Mittal R et al. *Phys. Rev. B* **78** 104514 (2008); arXiv:0807.3172
103. Higashitaniguchi S et al., arXiv:0807.3968
104. Fukuda T et al. *J. Phys. Soc. Jpn.* **77** 103715 (2008); arXiv:0808.0838
105. Zbiri M et al., arXiv:0807.4429
106. Zhao J et al. *Phys. Rev. Lett.* **101** 167203 (2008); arXiv:0808.2455
107. Ewings R A et al., arXiv:0808.2836
108. Lebègue S *Phys. Rev. B* **75** 035110 (2007)
109. Boeri L, Dolgov O V, Golubov A A *Phys. Rev. Lett.* **101** 026403 (2008); arXiv:0803.2703
110. Mazin I I et al. *Phys. Rev. Lett.* **101** 057003 (2008); arXiv:0803.2740
111. Xu G et al. *Europhys. Lett.* **82** 67002 (2008)
112. Shein I R, Ivanovskii A L *Pis'ma Zh. Eksp. Teor. Fiz.* **88** 115 (2008); [*JETP Lett.* **88** 107 (2008)]; arXiv:0806.0750
113. Singh D J *Phys. Rev. B* **78** 094511 (2008); arXiv:0807.2643
114. Ma F, Lu Z-Y, Xiang T, arXiv:0806.3526
115. Shein I R, Ivanovskii A L *Pis'ma Zh. Eksp. Teor. Fiz.* **88** 377 (2008) [*JETP Lett.* **88** (5) (2008)]
116. Subedi A et al. *Phys. Rev. B* **78** 134514 (2008); arXiv:0807.4312
117. Nekrasov I A, Pchelkina Z V, Sadovskii M V *Pis'ma Zh. Eksp. Teor. Fiz.* **87** 647 (2008) [*JETP Lett.* **87** 560 (2008)]; arXiv:0804.1239
118. Nekrasov I A, Pchelkina Z V, Sadovskii M V *Pis'ma Zh. Eksp. Teor. Fiz.* **88** 155 (2008) [*JETP Lett.* **88** 144 (2008)]; arXiv:0806.2630
119. Nekrasov I A, Pchelkina Z V, Sadovskii M V *Pis'ma Zh. Eksp. Teor. Fiz.* **88** 621 (2008) [*JETP Lett.* **88** 543 (2008)]; arXiv:0807.1010
120. Nekrasov I A, Pchelkina Z V, Sadovskii M V *Pis'ma Zh. Eksp. Teor. Fiz.* **88** 777 (2008) [*JETP* **88** (10) (2008)]; arXiv:0810.3377
121. Andersen O K *Phys. Rev. B* **12** 3060 (1975); Gunnarsson O, Jepsen O, Andersen O K *Phys. Rev. B* **27** 7144 (1983); Andersen O K, Jepsen O *Phys. Rev. Lett.* **53** 2571 (1984)
122. Goshchitskii B N, Kozhevnikov V L, Sadovskii M V *Int. J. Mod. Phys. B* **2** 1331 (1988)
123. Kuroki K et al. *Phys. Rev. Lett.* **101** 087004 (2008)
124. Chong S V, Mochiji T, Kadowaki K, arXiv:0808.0288
125. Yang J et al., arXiv:0809.3582
126. Shein I R, Ivanovskii A L, arXiv:0810.3498
127. Raghu S et al. *Phys. Rev. B* **77** 220503(R) (2008); arXiv:0804.1113
128. Cao C, Hirschfeld P J, Cheng H-P *Phys. Rev. B* **77** 220506(R) (2008); arXiv:0803.3236
129. Kuroki K et al., arXiv:0803.3325
130. Korshunov M M, Eremin I *Phys. Rev. B* **78** 140509(R) (2008); arXiv:0804.1793
131. Liu C et al., arXiv:0806.2147
132. Yang L X et al., arXiv:0806.2627
133. Liu C et al., arXiv:0806.3453
134. Liu H et al., arXiv:0806.4806
135. Zhao L et al. *Chinese Phys. Lett.* **25** 4402 (2008); arXiv:0807.0398
136. Ding H et al. *Europhys. Lett.* **83** 47001 (2008); arXiv:0807.0419
137. Wray L et al., arXiv:0808.2185
138. Zhang Y et al., arXiv:0808.2738
139. Zabolotnyy V B et al., arXiv:0808.2454
140. Evtushinsky D V et al., arXiv:0809.4455
141. Sato T et al., arXiv:0810.3047
142. Damaselli A, Hussain Z, Shen Z-X *Rev. Mod. Phys.* **75**, 473 (2003)
143. Sebastian S E et al. *J. Phys. Condens. Matter* **20** 422203 (2008); arXiv:0806.4726
144. Coldea A I et al., arXiv:0807.4890
145. Metzner W, Vollhardt D *Phys. Rev. Lett.* **62** 324 (1989)
146. Vollhardt D, in *Correlated Electron Systems* (Ed. V J Emery) (Singapore: World Scientific, 1993) p. 57
147. Pruske Th, Jarrell M, Freericks J K *Adv. Phys.* **44** 187 (1995)
148. Izyumov Yu A *Usp. Fiz. Nauk* **165** 403 (1995) [*Phys. Usp.* **38** 385 (1995)]
149. Georges A et al. *Rev. Mod. Phys.* **68** 13 (1996)
150. Kotliar G, Vollhardt D *Phys. Today* **57** (3) 53 (2004)
151. Kotliar G et al. *Rev. Mod. Phys.* **78** 865 (2006)
152. Held K *Adv. Phys.* **56** 829 (2007)
153. Haule K, Singh J H, Kotliar G *Phys. Rev. Lett.* **100** 226402 (2008); arXiv:0803.1279
154. Shorikov A O et al., arXiv:0804.3283
155. Anisimov V I et al., arXiv:0807.0547
156. Miyake T et al., arXiv:0808.2442
157. Anisimov V I et al., arXiv:0810.2629
158. Aryasetiawan F et al. *Phys. Rev. B* **70** 195104 (2004)
159. Miyake T, Aryasetiawan F *Phys. Rev. B* **77** 085122 (2008)
160. Anisimov V I, Gunnarsson O *Phys. Rev. B* **43** 7570 (1991)
161. Kurmaev E Z et al., arXiv:0805.0668
162. Yildirim T *Phys. Rev. Lett.* **101** 057010 (2008); arXiv:0804.2252
163. Mazin I I et al. *Phys. Rev. B* **78** 085104 (2008); arXiv:0806.1869
164. Mazin I I, Johannes N D *Nature Phys.* **5** 141 (2009); arXiv:0807.3737
165. Moskalenko V A, Palistrant M E, Vakalyuk V M *Usp. Fiz. Nauk* **161** (8) 155 (1991) [*Sov. Phys. Usp.* **34** 717 (1991)]

166. Barzykin V, Gor'kov L P *Pis'ma Zh. Eksp. Teor. Fiz.* **88** 142 (2008) [*JETP Lett.* **88** 131 (2008)]; arXiv:0806.1933
167. Keldysh L V, Kopaev Yu V *Fiz. Tverd. Tela* **6** 2791 (1964) [*Sov. Phys. Solid State* **6** 2219 (1965)]
168. Kozlov A N, Maksimov L A *Zh. Eksp. Teor. Fiz.* **49** 1284 (1965) [*Sov. Phys. JETP* **22** 889 (1966)]
169. Halperin B I, Rice T M, in *Solid State Physics* (Eds F Seitz, D Turnbull, H Ehrenreich) Vol. 21 (New York: Academic Press, 1968) p. 115
170. Kopaev Yu V *Trudy Fiz. Inst. Akad. Nauk SSSR* **86** 3 (1975)
171. Volkov B A *Trudy Fiz. Inst. Akad. Nauk SSSR* **104** 3 (1978)
172. Volovik G E, Gor'kov L P *Pis'ma Zh. Eksp. Teor. Fiz.* **39** 550 (1984) [*JETP Lett.* **39** 674 (1984)]
173. Volovik G E, Gor'kov L P *Zh. Eksp. Teor. Fiz.* **88** 1412 (1985) [*Sov. Phys. JETP* **61** 843 (1985)]
174. Parker D et al. *Phys. Rev. B* **78** 134524 (2008); arXiv:0807.3729
175. Allen P B, Dynes R C *Phys. Rev. B* **12** 905 (1975)
176. Eschrig H, arXiv:0804.0186
177. Bhoi D, Mandal P, Choudhury P *Supercond. Sci. Technol.* **21** 125021 (2008); arXiv:0808.2695
178. Allen P B, Pickett W E, Krakauer H *Phys. Rev. B* **37** 7482 (1988)
179. Liu R H et al., arXiv:0810.2694
180. Qi X-L et al., arXiv:0804.4332
181. Chubukov A V, Efremov D, Eremin I *Phys. Rev. B* **78** 134512 (2008); arXiv:0807.3735
182. Ginzburg V L, Kirzhnits D A (Eds) *Problema Vysokotemperaturnoi Sverkhprovodimosti* (High-Temperature Superconductivity) (Moscow: Nauka, 1977) [Translated into English (New York: Consultants Bureau, 1982)]